Kv1.3 channels modulate human vascular smooth muscle cells proliferation independently of mTOR signalling pathway

Pilar Cidad[1,$], Eduardo Miguel-Velado[1,$], Christian Ruiz-McDavitt[1], Esperanza Alonso[1], Laura Jiménez-Pérez[1], Agustín Asuaje[1], Yamila Carmona[1], Daniel García-Arribas[1], Javier López[2], Yngrid Marroquín[3], Mirella Fernández[2], Mercè Roqué[4], M. Teresa Pérez-García[1,#] and José Ramón López-López[1,#].

[1]Departamento de Bioquímica y Biología Molecular y Fisiología e Instituto de Biología y Genética Molecular (IBGM), Universidad de Valladolid y CSIC, Valladolid, Spain

[2]Servicio de Cardiología y Cirugía Cardíaca y [3]Servicio de Nefrología, Hospital Clínico Universitario, Valladolid, Spain

[4]Servicio de Cardiología. Institut Clinic del Tòrax, Hospital Clinic, IDIBAPS, Universidad de Barcelona, Barcelona, Spain

[$] equal contributors

[#] shared last authorship

Correspondence:

Dr. M. Teresa Pérez-García

Departamento de Bioquímica y Biología Molecular y Fisiología

Universidad de Valladolid

Edificio IBGM, c/ Sanz y Forés s/n

47003 Valladolid (SPAIN)

Phone: 34 983 184590

Fax: 34 983 184800

e-mail: tperez@ibgm.uva.es

Word count (excluding references): 6002

ABSTRACT

Phenotypic modulation (PM) of vascular smooth muscle cells (VSMCs) is central to the process of intimal hyperplasia which constitutes a common pathological lesion in occlusive vascular diseases. Changes in the functional expression of Kv1.5 and Kv1.3 currents upon PM in mice VSMCs have been found to contribute to cell migration and proliferation. Using human VSMCs from vessels in which unwanted remodelling is a relevant clinical complication, we explored the contribution of the Kv1.5 to Kv1.3 switch to PM. Changes in the expression and the functional contribution of Kv1.3 and Kv1.5 channels were studied in contractile and proliferating VSMCs obtained from human donors. Both a Kv1.5 to Kv1.3 switch upon PM and an anti-proliferative effect of Kv1.3 blockers on PDGF-induced proliferation were observed in all vascular beds studied. When investigated the signalling pathways modulated by the blockade of Kv1.3 channels, we found that anti-proliferative effects of Kv1.3 blockers on human coronary artery VSMCs were occluded by selective inhibition of MEK/ERK and PLCγ signalling pathways, but were unaffected upon blockade of PI3K/mTOR pathway. The temporal course of the anti-proliferative effects of Kv1.3 blockers indicates that they have a role in the late signalling events essential for the mitogenic response to growth factors. These findings establish the involvement of Kv1.3 channels in the PM of human VSMCs. Moreover, as current therapies to prevent restenosis rely on mTOR blockers, our results provide the basis for the development of novel, more specific therapies.

Key words: Kv1.3 channels, Vascular Smooth Muscle Cell proliferation, phenotypic switch, vascular remodeling, cell signaling.

INTRODUCTION

The cellular responses to vascular injury lead to clinical events such as atherosclerosis, hypertension and restenosis. One common feature of these lesions is the proliferation of vascular smooth muscle cells (VSMCs). While VSMCs proliferation plays a key role in the development and homeostasis of blood vessels, it also contributes to the pathogenesis of vascular diseases such as hypertension and restenosis [31]. Aside from the complications related to acute rejection, heart allograft vascular disease is a major complication determining long-term survival after heart transplantation. In spite of the improvements in prevention and treatment, up to 50% of the patients undergoing heart transplantation are diagnosed of allograft vasculopathy within 10 years [38]. This condition represents also the most common complication after percutaneous vascular interventions and stent implantation. In all these pathologies, dedifferentiated VSMCs are the major cellular component of the thickened vessel [5].

Proliferation of VSMC occurs in response to mitogens produced by platelets, activated T-cells, endothelial cells, macrophages and VSMCs themselves, including vasoactive agents (angiotensin II, endothelin [15] [20]), cytokines such as interleukine I [19] and growth factors such as platelet-derived growth factor (PDGF) [31]. Mechanistically, mitogens can activate intrinsic protein tyrosine kinase receptors (such as PDGF and EGF) or G-protein-coupled receptors (endothelin-I, angiotensin-II). In both cases, subsequent signalling via mitogen-activated protein kinases (MAPKs) leads to regulation of gene expression and cell cycle re-entry to stimulate cell proliferation [3,22,35].

PDGF-BB is the most potent known chemoattractant for VSMCs. Upon PDGF binding, the receptor tyrosine kinase autophosphorylates, creating docking sites for recruitment of SH2 domain-containing signalling molecules. Within minutes, many signalling modules are engaged, including several MAPKs, the phospholipase C gamma (PLCγ) and phosphoinositide 3 kinase (PI3K) [17,29,40].

K^+ channels have been implicated in proliferation of a large number of cell types since the initial description of a voltage-dependent K^+-channel (Kv1.3) mediating proliferation in T cells [9]. Subsequently, a plethora of K^+ channels have been linked to migration and proliferation in numerous non-excitable tissues, including cancer cells, T-lymphocytes, endothelial cells and VSMCs [1,11,32,43]. Several K^+ channels, including KCa3.1, Kv3.4 and Kv1.3 have been shown to associate with VSMC proliferation [8,24,27,41]. While in some cases this association depends on their ion-conducting properties, in others it is unknown how their activity is linked to proliferation. In fact, there are some studies indicating that the effect of ion channels on cell proliferation relies on non-conducting properties of the channel proteins [7,16,28].

In our previous work, we postulate that Kv1.3/Kv1.5 ratio can be considered as a landmark of VSMCs phenotype, because proliferation of VSMCs from several vascular beds in mice associates with a Kv1.5 to Kv1.3 channel switch [7]. Here, we explore if this role of Kv1.3 in the VSMCs phenotypic modulation (PM) is also present in human vessels, and we investigate the signalling cascade linking Kv1.3 expression to increased VSMCs proliferation. We confirm the anti-proliferative effect of Kv1.3 blockers in human VSMCs. The effects of Kv1.3 blockers can be occluded by selective inhibition of MEK/ERK and PLCγ pathways, but were additive to those of PI3K/mTOR blockers, opening interesting possibilities for the use of Kv1.3 blockers in the prevention and treatment of occlusive diseases.

MATERIALS AND METHODS

Sample collection

Human uterine (hUA), renal (hRA) and coronary arteries (hCA) and saphenous veins (hSV) belonging to the COLMAH collection of the HERACLES network (http://www.redheracles.net/plataformas/en_coleccion-muestras-arteriales-humanas.html) were obtained from donors at the Clinic Hospitals of Barcelona and Valladolid. Vessels were divided in two pieces, one was placed in RNAlater (Ambion) for RNA extractions and the other in a Dulbecco's modified Eagle's medium (DMEM), for cell isolation. Samples kept at 4 ºC were received within 24 hours after intervention. Cultured VSMCs were obtained from explants of the vessels as described elsewhere [27]

mRNA and protein determinations

RNA from tissue homogenates and from cultured VSMCs was isolated with TRIzol Reagent and reverse transcribed. mRNA levels were determined by real-time qPCR with TaqMan® Gene Expression Assays (Applied Biosystems) on a Rotor-Gene 3000 instrument (Corbett Research) using the $2^{-\Delta\Delta Ct}$ relative quantification method [26]. Western-blot of protein lysates obtained from vascular tissues (contractile VSMCs) or primary cultures (proliferative VSMCs) were used for protein detection. Quantification was carried out with the VersaDoc™ 4000 Image System (BioRad) with chemiluminescence reagents

Electrophysiological methods and intracellular calcium measurements

Ionic currents were recorded at room temperature (20-25ºC) using the whole-cell configuration of the patch-clamp technique as previously described [27,30]. Membrane potential (V_M) measurements were obtained at RT using the perforated-patch technique [39]. For intracellular calcium measurements, hCA VSMCs were loaded with Fluo-4-AM (Molecular Probes, Invitrogen, Oregon, USA). Changes in fluorescence in response to the indicated stimuli were analyzed with Imaging Workbench 4.0 image software.

Proliferation assays

Proliferation was determined using a commercial kit (Click-iT® EdU Imaging Cell Proliferation Assay, Invitrogen). VSMCs at passages 3-8 were seeded onto 12 mm poly-l-lysine coated coverslips and synchronized in serum-free (SF) medium during 48 h before adding the proliferative stimulus (alone or in combination with specific inhibitors) during 24 h.

An expanded material and methods section with detailed protocols can be found in the Online Suplemental Resource.

RESULTS

The ratio of Kv1.3 to Kv1.5 mRNA can define the VSMC phenotype

In mice VSMCs, PM associates with a consistent change in the Kv1.3 to Kv1.5 ratio [7]. Here, we determined the relative abundance of Kv1.3 and Kv1.5 mRNA in VSMCs obtained from several human vascular beds, both in contractile (*Tissue*) and in proliferative phenotype (*Culture*). mRNA expression levels of another K^+ channel (the intermediate conductance Ca^{2+}-activated K^+ channel, KCa3.1) previously reported to associate with VSMCs proliferation [24,42] were also explored. Figure 1a shows mRNA levels in VSMCs from human saphenous veins (hSV), coronary (hCA) and renal arteries (hRA). Kv1.5 mRNA expression was predominant in all vascular beds in the contractile phenotype, decreasing dramatically upon PM. Otherwise, Kv1.3 and

KCa3.1 mRNA levels were significantly lower and the changes upon PM smaller. Similar data has been found in human uterine artery (hUA)[27]. Nevertheless, when these data are represented as Kv1.3/ Kv1.5 ratio ($2^{-\Delta\Delta Ct}$), it is evident that a clear switch from Kv1.5 to Kv1.3 upon PM is conserved in all vascular beds explored. This ratio is expressed in Figure 1b in a logarithmic scale, so that negative values reflect a higher expression of Kv1.5 mRNA whilst positive values reflect a higher expression of Kv1.3 mRNA. In all cases, Kv1.3 became the predominant Kv1 channel expressed in cultured VSMCs, mainly due to the dramatic decrease of Kv1.5 mRNA upon PM (Figure 1c).

Changes in mRNA Kv1.3/Kv1.5 ratio upon PM correlate with changes in functional channel protein expression

We next explored the protein expression of Kv1.3 and Kv1.5 channels. Protein extracts obtained from hRA VSMCs, both in contractile (Tissue) and proliferating (Cultured) phenotype were used for immunoblots with anti-Kv1.3 and anti-Kv1.5 (Figure 2a). The expression of Kv1.5 protein significantly decreased in cultured VSMCs, in agreement with the mRNA expression levels. However, changes in Kv1.3 protein (almost not-detectable in contractile VSMCs and robustly expressed in cultured VSMCs) were not anticipated from the mRNA expression data.

Electrophysiological studies in VSMCs obtained from hRA allowed functional characterization of the channels (Figure 2b-d). Whole cell patch-clamp experiments were carried out in VSMCs freshly dispersed (contractile) or from VSMCs maintained in primary culture. Kv currents were elicited by depolarizing pulses to +40 mV, and Kv1.3 and Kv1.5 contribution was estimated as the fraction of current sensitive to the selective blockers 5-(4-phenoxybutoxy) psoralen (PAP-1) or diphenyl phosphine oxide (DPO) respectively[7,36]. Representative experiments (Figure 2b) and average data (Part C) are depicted. Kv1.5 currents represented a large fraction of the Kv currents elicited in contractile VSMCs, being almost absent in cultured VSMCs. On the contrary, the fraction of PAP-1 sensitive currents (Kv1.3) increased from contractile to cultured VSMCs. This increase remains when Kv1.3 currents are normalized by cell capacitance (Figure 2d), in spite of the bigger size of proliferating VSMCs (43.4 ± 4.0 pF vs. 29.27 ± 2.34 pF of the freshly dissociated cells), indicating an increased expression of Kv1.3 channels in the plasma membrane of proliferative VSMCs. In addition, we explored whether Kv1.3 currents contribute to set the resting membrane potential (E_M) in cultured VSMCs with current clamp experiments (Figure 2e). We found that 100 nM PAP-1 induced small, consistent depolarization, averaging 2.48 ± 0.3 mV (n=6). Similar depolarizations were obtained in hCA cultured VSMCs (2.62 ± 0.35 mV, n=12).

Comparable results were obtained in hCA and hSV (Online Supplemental Resource, Figure I). In all cases the almost absence of DPO-sensitive currents and the large contribution of Kv1.3 channels to total Kv currents in cultured VSMCs were evident.

Exploring the contribution of changes in Kv1.3/Kv1.5 ratio to PM

We hypothesized that the Kv1.5 to Kv1.3 switch could be a relevant event needed to facilitate the acquisition of the proliferative and/or migratory capabilities of the PM. In explants from hRA, the switch on mRNA expression could be observed as soon as after 3 days in culture, becoming more pronounced at 7 days (Figure 3a). No evident proliferation and migration could be observed at these times, suggesting that the Kv1 switch is needed for the PM and that the changes in their expression levels are modulated by the mitogenic signals initiating PM.

KCa3.1 channels in coronary VSMCs are upregulated upon PM as a consequence of the proliferative stimulus[37,41]. To explore if this was also the case for Kv1.3 channels, we analyzed the changes in mRNA expression levels upon treatment of VSMCs cultures with 20% FBS (Figure 3b) or 100 ng/ml PDGF (Figure 3c). KCa3.1

mRNA increased both in hRA and hSV VSMCs upon stimulation with FBS or PDGF. However, Kv1.3 mRNA expression did not change significantly. These data point to a fundamental difference in the regulation of both ion channels during PM. Whilst KCa3.1 channels seem to be regulated transcriptionally, Kv1.3 increased protein expression in the proliferative phenotype (Figure 2) requires an alternate explanation.

Selective blockade of Kv1.3 currents inhibits proliferation

The increased functional expression of Kv1.3 currents in cultured VSMCs suggests a link between the channel and the establishment and/or maintenance of the proliferative phenotype. To explore this possibility we have tested the effect of 100 nM PAP-1 and 10 nM Margatoxin (MgTx) on the FBS-induced proliferation in VSMCs obtained from 4 different human vessels (Figure 4a). In all cases we found a significant decrease on the rate of FBS-induced proliferation in the presence of Kv1.3 blockers, suggesting a functional association of Kv1.3 expression with PM. To further investigate the signaling pathways linking the functional expression of Kv1.3 channels to VSMC proliferation, we explored the effects of Kv1.3 blockade on the proliferation induced by specific growth factors such as PDGF or ATII (Figure 4b). ATII (1 µM) was a proliferative stimulus not as potent as PDGF (100 ng/ml). However, the inhibitory effect of 100 nM PAP-1 was the same in the two conditions, suggesting a common signalling pathway. Interestingly, when 100 ng/ml PDGF was used as the proliferative stimulus in VSMCs, proliferation rates were comparable to those obtained with 5-20% FBS (see Online Supplemental Resource, Figure II), but the effect of 100 nM PAP-1 inhibiting proliferation was much stronger. Although this difference was particularly evident in hCA (~20% inhibition with FBS vs. ~60% inhibition with PDGF), similar results were obtained when VSMCs from other vascular beds were studied (Figure 4c). Figure 4d shows the summary data obtained from hRA VSMCs when exploring the effect of different K^+ channel blockers on PDGF-induced proliferation. Both PAP-1 (100nM) and MgTx (10 nM) show a similar inhibitory effect. A marked inhibition was also observed with the selective KCa3.1 blocker TRAM-34 (100 nM). The specific role of these two channels (Kv1.3 and KCa3.1) in the proliferative phenotype is supported by the lack of effect of selective blockers of BK_{Ca} channels, even though BK_{Ca} currents are present in cultured VSMCs (data not shown).

Kv1.3 effects on proliferation are mediated by ERK1/2 and PLCγ signaling pathway

We sought to identify the signaling pathway(s) contributing to PDGF-induced proliferation that can be affected by Kv1.3 blockade. We determined the effect on proliferation of selective blockers of the different pathways activated by PDGF in hCA VSMCs. No effect on proliferation was observed upon blockade of JNK or p38 kinases with 1 µM SP600125 or 20 µM SB203580 respectively (Figure 5a). On the contrary, blockers of the ERK1/2, PI3K/mTOR and PLCγ pathways were effective inhibiting VSMCs proliferation. In these cases, we also studied if some additional effect could be observed upon selective blockade of Kv1.3 channels with PAP-1 (100 nM) or MgTx (10 nM). The effect of PAP-1 or MgTx was occluded in the presence of either ERK1/2 blockers or PLCγ blockers, suggesting that the pro-proliferative effects of Kv1.3 are mediated by these two pathways. On contrast, the effect of 100 nM PAP-1 is still present when either PI3K or mTOR were inhibited. In fact, the percent inhibition was not significantly changed when the proliferation obtained with the different PI3K/mTOR blockers were taken as control (51,5% in control vs. 51,2% in the presence of LY294002, 44% with rapamicin 1 nM and 58% with Everolimus 0.1 nM) suggesting independent pathways and strictly additive effects.

Finally, the inhibitory effects of PD98059 (ERK1/2) and U73122 (PLCγ) were not additive, suggesting that these two signaling pathways converge in a common effector that could be the target of Kv1.3. However, the PI3K/mTOR pathway was clearly

independent from ERK1/2 or PLCγ, since 0.1 nM Everolimus clearly potentiated the effect of ERK1/2 and PLCγ blockers.

The additive effect of Kv1.3 blockers and mTOR blockers was explored in more detail by analyzing the dose-response curve for everolimus inhibition of PDGF-induced proliferation, either alone or in the presence of 100 nM PAP-1 (Figure 5c). PAP-1 increased the inhibitory effect of everolimus at all the concentrations tested, with a similar effect at all the concentrations of everolimus, suggesting again independent mechanisms. 100 nM PAP-1 had submaximal effects on proliferation, as illustrated in the PAP-1 dose-response curve obtained in hCA VSMCs (Online Supplemental Resource, Figure III).

When exploring the contribution of KCa3.1 channels in a series of similar experiments, we found that, as in hRA (figure 4d) 100 nM TRAM-34 inhibited PDGF-induced proliferation in hCA VSMCs (Figure 6). However, this inhibitory effect of TRAM-34 was not additive to the effect of 100nM PAP-1 (or 10nM MgTx, not shown), suggesting a common effector . Finally, in a similar fashion to the effects of Kv1.3 blockers, the effect of TRAM-34 seems to be mediated by signaling through ERK1/2 (as previously described in A7r5 VSMCs, [37]) but not through PI3K/mTOR pathways. We conclude that both Kv1.3 and KCa3.1 channels contribute to VSMCs through some common effectors, indicating some redundancy on the mechanisms controlling VSMCs proliferation.

Exploring the mechanisms involved in the anti-proliferative effect of Kv1.3 blockers

Data obtained in hCA VSMCs suggested that the effects of Kv1.3 channels on PDGF-induced proliferation were mediated through some common effector of the ERK1/2 and the PLCγ signaling pathways. In order to identify this effector, we explored the effects of PAP-1 treatment on some well-known early events taking place upon activation of these signaling pathways, namely the phosphorylation of ERK1/2 or the increase in $[Ca^{2+}]_i$ upon PDGF activation of PLCγ (Figure 7). ERK1/2 phosphorylation was evaluated by immunoblot analysis. pERK levels peaked around 10 min after PDGF stimulation, decreasing to levels close to basal ones for PDGF incubations up to 24h (Figure 7a). No significant differences in the levels of pERK production or in the temporal pattern were observed in VSMCs pretreated with 100 nM PAP-1.

The possible effect of Kv1.3 blockers on the initial steps of PDGF activation of PLCγ was studied by determining the changes in $[Ca^{2+}]_i$ in response to acute application of PDGF. A short pulse of PDGF elicited a transient increase of $[Ca^{2+}]_i$ that was completely abolished by preincubation with the PLCγ blocker U73122, but unaffected by the presence of either MgTx or PAP-1 (figure 7b). Also consistent with these observations, the up regulation of cyclin D, one of the main growth factor-induced events in early G1, is not affected by treatment with 100 nM PAP, but is blunted with incubation with everolimus as previously described [3] (figure 7c). In fact, short (30 min) incubations with PDGF had a minimal proliferative effect when compared with long (24h) incubations (Figure 8a), suggesting that ERK1/2 phosphorylation and $[Ca^{2+}]_i$ increase may not suffice to promote PDGF-induced VSMC proliferation. In agreement with this observation, the inhibitory effect of PAP-1 on PDGF-induced hCA proliferation is not reduced when PAP-1 is added 30 min or 1h after PDGF application, being only significantly different when its application is delayed several hours (figure 8b). Altogether, these data exclude a role of Kv1.3 channel at the initial steps of PDGF signaling cascade

DISCUSION

The characterization of the mechanisms involved in the PM of VSMCs is a relevant issue with important clinical implications, as the cellular responses to vascular injury are important events in the formation of neointima in pathological states such as hypertension, atherosclerosis and allograft vasculopathy. The knowledge of the signal transduction pathways controlling VSMCs activation and PM may provide additional points of control that can represent novel therapeutical opportunities. Kv1.3 channels could constitute one of those new therapeutical targets, as we show evidence indicating that the pro-proliferative role of Kv1.3 previously described in mice [8] can also be observed in human VSMCs obtained from different vascular beds. Moreover, the search for some mechanistic insights aimed to identify the signalling pathways involved in the effect of Kv1.3 in proliferation, highlights nontrivial therapeutical opportunities.

The contribution of Kv1.3 channels to human VSMCs proliferation seems to be a conserved, vascular bed-independent mechanism, as it could be observed in all vessels studied. Interestingly, unwanted remodelling is a relevant issue in most of the vascular beds studied.

PM in human VSMCs associates with a change in mRNA Kv1.3/Kv1.5 ratio (Figure 1). This change is mainly due to the large decrease of Kv1.5 transcripts (the most abundant Kv1 transcript in contractile VSMCs [6,7,30]) on proliferating cells. The switch in the ratio is an early event in the process of VSMC dedifferentiation, as it can be observed before VSMC proliferation is evident. However, in spite of Kv1.3 increased functional expression in cultured VSMCs, Kv1.3 mRNA expression is not significantly different between contractile and proliferating VSMCs, suggesting that regulation of Kv1.3 protein expression is not mediated by transcriptional mechanisms. We also studied the changes in the expression of KCa3.1 channels, since they have been previously implicated in the control of VSMCs proliferation both in vivo and in vitro [1,24,42]. We found variable PM associated changes in KCa3.1 expression: increase in proliferating hRA and hCA VSMCs and no changes in hSV or hUA VSMCs [27]. However, in contrast to Kv1.3, KCa3.1 expression was up-regulated in the presence of proliferating stimuli such as FBS and PDGF (Figure 3, [37]), revealing a fundamental difference in the modulation of the expression of those two channels.

The functional expression of Kv1.3 channels was explored electrophysiologically, and their contribution to proliferation was demonstrated by the anti-proliferative effects of the selective blockers PAP-1 and MgTx. Our data indicate that the up-regulated functional expression of Kv1.3 channels contributes to VSMC proliferation. An alternative explanation could be that the relevant change for PM is Kv1.5 downregulation, so that VSMC proliferation will not take place if Kv1.5 decrease is prevented. This idea is consistent with the observation that while Kv1.3 over-expression is able to increase HEK293 cells proliferation, Kv1.5 over-expression significantly decreases it [7]. However, more research will be needed to determine whether in native VSMCs the functional expression of Kv1.5 channels is linked to anti-proliferative signalling or if it is the formation of Kv1.3/Kv1.5 heteromultimers what occludes the pro-proliferative signalling pathways mediated by Kv1.3 channels.

Selective blockade of Kv1.3 channels was able to inhibit FBS-induced proliferation in all human VSMCs tested, albeit with different potency. The anti-proliferative effect of Kv1.3 blockers was more homogeneous when cells were stimulated with a specific mitogen such as PDGF. PDGF activates multiple signalling pathways in VSMCs including Src, PLCγ, Ras, PI3K/mTOR and MAPKs, which associate to cellular responses such as migration, proliferation and gene expression (reviewed in [18,29]). Most of these signalling pathways are present in VSMCs and activated by PDGF.

However, despite (and possibly because of) the diversity of this complex network of signals, the precise association of each pathway to a particular cellular effect is incompletely understood. The possibility of crosstalk and compensation between pathways, as well as their different contribution in different cell types also complicates their characterization [29,40]. We found a contribution to VSMC proliferation of PI3K/mTOR, PLCγ and ERK1/2 signalling, in agreement with previous reports [14,25,44]. Also in agreement with our data , p38 and JNK kinases have been previously found to have a minor contribution to VSMC proliferation, being more involved in VSMC migration and remodelling-related gene expression [44].

The activity of Kv1.3 channels modulates proliferation acting on ERK1/2 and PLCγ signalling pathways, as inhibition of proliferation by Kv1.3 blockers was occluded in the presence of selective inhibitors of these pathways, suggesting competition for the same site of action. We confirm this observation using different blockers with unrelated mechanisms of action or even different molecular target. Similarly, the fact that the effects of PAP-1 on proliferation were always reproduced by another structurally unrelated blocker such as MgTx [13,36] supports the interpretation that their antiproliferative effect is due to Kv1.3 channel inhibition. We also found that blockade of KCa3.1 inhibits VSMCs in all human vascular beds, but does not potentiate the effect Kv1.3 channels blockers. These findings suggest in the one hand the presence of several alternate signalling pathways to ensure the activation of VSMC proliferation upon PM, and in the other that the control of either E_M or $[Ca^{2+}]_I$, or both, through the activation of any of these K^+ channels, is an important element of the signaling pathway leading to VSMC proliferation.

Regarding the downstream signalling pathways involved in cell-cycle progression, previous reports demonstrate that there are two waves of growth factor-dependent signalling events required for a proliferative response. One is an acute signalling, that occurs immediately and subsides even in the continuous presence of the growth factor [22], but is insufficient for cell cycle progression [21,34]. The second wave overlaps temporally with the cell cycle program and may be directly responsible for engaging it, as PI3K/mTOR, PKC and Ras activity during this second wave are essential for the mitogenic response to growth factors [22]. The pathways activated by these two waves may not be mutually exclusive, as there is a common signaling cascade that involves the temporally coordinated input of several effectors [21,22], being the cellular responses depending on the timing, the duration and the intensity of these signals [23,33,34]. Within this scheme, our data suggest that Kv1.3 channels play a role in that second wave of signaling events, as the same inhibition was found when PAP-1 is applied together with PDGF or 30 min or 1 h later (when all early events had taken place) while no significant inhibition was found when application was delayed for 12h (when the second wave is over). Moreover, short time (30 min) application of PDGF only elicited a weak proliferative response not affected by PAP-1 (Figure 8b).

The role of E_M in VSMC proliferation is an interesting issue. It has been postulated that K^+ channel inhibition depolarizes the cells, decreasing the driving force for Ca^{2+} entry, and the subsequent decrease of $[Ca^{2+}]$ could inhibit proliferation. However, we found that Kv1.3 blockade depolarize the membrane (Figure 2b), but does not affect Ca^{2+} transients (Figure 7b and Online Supplemental Resource, Figure IV). In the light of these observations, an alternative hypothesis could be that Kv1.3 modulates proliferation acting as a voltage sensor through cell cycle progression, coupled to ERK1/2 or PLCγ pathways [7]. Further experiments, measuring E_M changes and/or $[Ca^{2+}]$ along G0/G1 to S phase progression in native VSMCs will contribute to clarify this aspect.

Interestingly, the pro-proliferative effect of Kv1.3 does not require PI3K/mTOR activation. This is a clear-cut result in our study. Both rapamycin and everolimus exhibit potent inhibition of growth factor-induced proliferation of lymphocytes and VSMCs, and have been extensively used for maintenance of immunosuppression after transplantation [12] and to prevent neointimal hyperplasia after balloon angioplasty and/or stenting [10,14]. In a similar fashion, Kv1.3 channels constitute a promising new anti-inflammatory drug target due to their roles in lymphocyte activation [4]. Kv1.3 is predominantly expressed in T cells and macrophages and is up-regulated in effector memory T cells, and Kv1.3 blockers have been proposed as novel therapies for the treatment of autoimmune diseases [2,36,43]. The present work provides a role for these channels in the modulation of human VSMCs proliferation, as we have demonstrate that they can serve also as therapeutical targets for the prevention and treatment of allograft vasculopathy. The fact that the anti-proliferative mechanisms involving Kv1.3 channel blockers and mTOR antagonist are additive represents a very interesting therapeutical opportunity.

FUNDING

Supported by grants from Ministerio de Economía y Competitividad, Instituto de Salud Carlos III (RIC RD12/0042/0006, Red Heracles), Ministerio de Ciencia e Innovación (BFU2010-15898 to MTPG), Junta de Castilla y León (VA094A11-2 to, JRLL) and Fondo de Investigaciones Sanitarias (FIS PI11/00225 to MR).

ACKNOWLEDGEMENTS

We thank Rodrigo de Pedro for excellent technical assistance

ETHICAL STANDARDS

For human samples, informed consent was given prior to inclusion. Protocols conforming the Declaration of Helsinki were approved by the Human Investigation Ethics Committees of the respective Hospitals.

All the experimental work performed complies with the Spanish legislation.

CONFLICT OF INTEREST

The authors declare that they have no conflict of interest.

Reference List

1. Beech DJ (2007) Ion channel switching and activation in smooth-muscle cells of occlusive vascular diseases. Biochemical Society Transactions 035:890-894

2. Beeton C, Wulff H, Standifer NE, Azam P, Mullen KM, Pennington MW, Kolski-Andreaco A, Wei E, Grino A, Counts DR, Wang PH et al (2006) Kv1.3

channels are a therapeutic target for T cell-mediated autoimmune diseases. Proc Natl Acad Sci U S A 103:17414-17419

3. Caglayan E, Vantler M, Lepp+ñnen O, Gerhardt F, Mustafov L, ten Freyhaus H, Kappert K, Odenthal M, Zimmermann WH, Tallquist MD and Rosenkranz S (2011) Disruption of Platelet-Derived Growth Factor-Dependent Phosphatidylinositol 3-Kinase and Phospholipase C γ1 Activity Abolishes Vascular Smooth Muscle Cell Proliferation and Migration and Attenuates Neointima Formation In Vivo. J Am Coll Cardiol 57:2527-2538

4. Cahalan MD, Chandy KG, DeCoursey TE and Gupta S (1985) A voltage-gated potassium channel in human T lymphocytes. The Journal of Physiology 358:197-237

5. Campbell GR and Campbell JH (1985) Smooth muscle phenotypic changes in arterial wall homeostasis: Implications for the pathogenesis of atherosclerosis. Exper Mol Pathol 42:139-162

6. Chen TT, Luykenaar KD, Walsh EJ, Walsh MP and Cole WC (2006) Key Role of Kv1 Channels in Vasoregulation. Circ Res 99:53-60

7. Cidad P, Jimenez-Perez L, Garcia-Arribas D, Miguel-Velado E, Tajada S, Ruiz-McDavitt C, Lopez-Lopez JR and Perez-Garcia MT (2012) Kv1.3 channels can modulate cell proliferation during phenotypic switch by an ion-flux independent mechanism. Arterioscler Thromb Vasc Biol 32:1299-1307

8. Cidad P, Moreno-Dominguez A, Novensa L, Roque M, Barquin L, Heras M, Perez-Garcia MT and Lopez-Lopez JR (2010) Characterization of ion channels involved in the proliferative response of femoral artery smooth muscle cells. Arterioscler Thromb Vasc Biol 30:1203-1211

9. DeCoursey TE, Chandy KG, Gupta S and Cahalan MD (1984) Voltage-Gated K+ Channels in Human Lymphocyte-T - A Role in Mitogenesis. Nature 307:465-468

10. Eisen HJ, Tuzcu EM, Dorent R, Kobashigawa J, Mancini D, Valantine-von Kaeppler HA, Starling RC, Sörensen K, Hummel M, Lind JM, Abeywickrama KH et al (2003) Everolimus for the Prevention of Allograft Rejection and Vasculopathy in Cardiac-Transplant Recipients. New Engl J Med 349:847-858

11. Erdogan A, Schaefer CA, Schaefer M, Luedders DW, Stockhausen F, Abdallah Y, Schaefer C, Most AK, Tillmanns H, Piper HM and Kuhlmann CR (2005) Margatoxin inhibits VEGF-induced hyperpolarization, proliferation and nitric oxide production of human endothelial cells. J Vasc Res 42:368-376

12. Formica Jr RN, Lorber KM, Friedman AL, Bia MJ, Lakkis F, Smith JD and Lorber MI (2004) The evolving experience using everolimus in clinical transplantation. Transplantation Proceedings 36:S495-S499

13. Garcia-Calvo M, Leonard RJ, Novick J, Stevens SP, Schmalhofer W, Kaczorowski GJ and Garcia ML (1993) Purification, characterization, and biosynthesis of margatoxin, a component of Centruroides margaritatus venom that selectively inhibits voltage-dependent potassium channels. J Biol Chem 268:18866-18874

14. Hafizi S, Mordi VN, Andersson KM, Chester AH and Yacoub MH (2004) Differential effects of rapamycin, cyclosporine A, and FK506 on human coronary artery smooth muscle cell proliferation and signalling. Vasc Pharmacol 41:167-176

15. Hafizi S, Wang X, Chester AH, Yacoub MH and Proud CG (2004) ANG II activates effectors of mTOR via PI3-K signaling in human coronary smooth muscle cells. Am J Physiol - Heart Circ Physiol 287:H1232-H1238

16. Hegle AP, Marble DD and Wilson GF (2006) A voltage-driven switch for ion-independent signaling by ether-a-go-go K+ channels. Proc Natl Acad Sci U S A 103:2886-2891

17. Heldin CH and Westermark B (1999) Mechanism of Action and In Vivo Role of Platelet-Derived Growth Factor. Physiol Rev 79:1283-1316

18. Hughes AD, Clunn GF, Refson J and Demoliou-Mason C (1996) Platelet-derived growth factor (PDGF): Actions and mechanisms in vascular smooth muscle. Gen Pharmacol 27:1079-1089

19. Isoda K, Shiigai M, Ishigami N, Matsuki T, Horai R, Nishikawa K, Kusuhara M, Nishida Y, Iwakura Y and Ohsuzu F (2003) Deficiency of interleukin-1 receptor antagonist promotes neointimal formation after injury. Circulation 108:516-518

20. Jia L, Wang R and Tang DD (2012) Abl regulates smooth muscle cell proliferation by modulating actin dynamics and ERK1/2 activation. Am J Physiol - Cell Physiol 302:C1026-C1034

21. Jones SM and Kazlauskas A (2001) Growth factor-dependent signaling and cell cycle progression. Febs Letters 490:110-116

22. Jones SM and Kazlauskas A (2001) Growth-factor-dependent mitogenesis requires two distinct phases of signalling. Nat Cell Biol 3:165-172

23. Jurek A, Heldin CH and Lennartsson J (2011) Platelet-derived growth factor-induced signaling pathways interconnect to regulate the temporal pattern of Erk1/2 phosphorylation. Cellular Signalling 23:280-287

24. Kohler R, Wulff H, Eichler I, Kneifel M, Neumann D, Knorr A, Grgic I, Kampfe D, Si H, Wibawa J, Real R et al (2003) Blockade of the Intermediate-Conductance Calcium-Activated Potassium Channel as a New Therapeutic Strategy for Restenosis. Circulation 108:1119-1125

25. Liou SF, Yeh JL, Liang JC, Chiu CC, Lin YT and Chen IJ (2004) Inhibition of Mitogen-Mediated Proliferation of Rat Vascular Smooth Muscle Cells by Labedipinedilol-A through PKC and ERK 1/2 Pathway. J Cardiovasc Pharmacol 44:539-551

26. Livak KJ and Schmittgen TD (2001) Analysis of relative gene expression data using real-time quantitative PCR and the 2(-Delta Delta C(T)) Method. Methods 25:402-408

27. Miguel-Velado E, Moreno-Dominguez A, Colinas O, Cidad P, Heras M, Perez-Garcia MT and López-López JR (2005) Contribution of Kv Channels to Phenotypic Remodeling of Human Uterine Artery Smooth Muscle Cells. Circ Res 97:1280-1287

28. Millership JE, Devor DC, Hamilton KL, Balut CM, Bruce JIE and Fearon IM (2011) Calcium-activated K+ channels increase cell proliferation independent of K+ conductance. Am J Physiol - Cell Physiol 300:C792-C802

29. Millette E, Rauch BH, Kenagy RD, Daum G and Clowes AW (2006) Platelet-Derived Growth Factor-BB Transactivates the Fibroblast Growth Factor

Receptor to Induce Proliferation in Human Smooth Muscle Cells. Trends in Cardiovasc Med 16:25-28

30. Moreno-Dominguez A, Cidad P, Miguel-Velado E, Lopez-Lopez JR and Perez-Garcia MT (2009) De novo expression of Kv6.3 contributes to changes in vascular smooth muscle cell excitability in a hypertensive mice strain. J Physiol 587:625-640

31. Owens GK, Kumar MS and Wamhoff BR (2004) Molecular regulation of vascular smooth muscle cell differentiation in development and disease. Physiol Rev 84:767-801

32. Pardo LA (2004) Voltage-Gated Potassium Channels in Cell Proliferation. Physiology 19:285-292

33. Roche S, Koegl M and Courtneidge SA (1994) The phosphatidylinositol 3-kinase alpha is required for DNA synthesis induced by some, but not all, growth factors. Proc Natl Acad Sci U S A 91:9185-9189

34. Roovers K and Assoian RK (2000) Integrating the MAP kinase signal into the G1 phase cell cycle machinery. Bioessays 22:818-826

35. Sabri A, Govindarajan G, Griffin TM, Byron KL, Samarel AM and Lucchesi PA (1998) Calcium- and Protein Kinase -Dependent Activation of the Tyrosine Kinase PYK2 by Angiotensin II in Vascular Smooth Muscle. Circ Res 83:841-851

36. Schmitz A, Sankaranarayanan A, Azam P, Schmidt-Lassen K, Homerick D, Hansel W and Wulff H (2005) Design of PAP-1, a selective small molecule Kv1.3 blocker, for the suppression of effector memory T cells in autoimmune diseases. Mol Pharmacol 68:1254-1270

37. Si H, Grgic I, Heyken WT, Maier T, Hoyer J, Reusch HP and K+Âhler R (2006) Mitogenic modulation of Ca2+-activated K+ channels in proliferating A7r5 vascular smooth muscle cells. Br J Pharmacol 148:909-917

38. Stehlik J, Edwards LB, Kucheryavaya AY, Benden C, Christie JD, Dipchand AI, Dobbels F, Kirk R, Rahmel AO and Hertz MI (2012) The Registry of the International Society for Heart and Lung Transplantation: 29th official adult heart transplant report--2012. J Heart Lung Transplant 31:1052-1064

39. Tajada S, Cidad P, Moreno-Domínguez A, Pérez-García MT and López-López JR (2012) High blood pressure associates with the remodelling of inward rectifier K^+ channels in mice mesenteric vascular smooth muscle cells. J Physiol 590:6075-6091

40. Tallquist M and Kazlauskas A (2004) PDGF signaling in cells and mice. Cytokine & Growth Factor Reviews 15:205-213

41. Tharp DL and Bowles DK (2009) The intermediate-conductance Ca2+ -activated K+ channel (KCa3.1) in vascular disease. Cardiovasc Hematol Agents Med Chem 7:1-11

42. Tharp DL, Wamhoff BR, Wulff H, Raman G, Cheong A and Bowles DK (2008) Local delivery of the KCa3.1 blocker, TRAM-34, prevents acute angioplasty-induced coronary smooth muscle phenotypic modulation and limits stenosis. Arterioscler Thromb Vasc Biol 28:1084-1089

43. Wulff H, Castle NA and Pardo LA (2009) Voltage-gated potassium channels as therapeutic targets. Nat Rev Drug Discov 8:982-1001

44. Zhan Y, Kim S, Yasumoto H, Namba M, Miyazaki H and Iwao H (2002) Effects of dominant-negative c-Jun on platelet-derived growth factor-induced vascular smooth muscle cell proliferation. Arterioscler Thromb Vasc Biol 22:82-88

FIGURE LEGENDS

Figure 1. mRNA expression levels of Kv1.3 and Kv1.5. a. Relative abundance of Kv1.3, Kv1.5 and KCa3.1 mRNA was determined in human saphenous veins, (hSV), coronary arteries, (hCA), and renal arteries, (hRA) both in contractile (*Tissue, open bars*) and in proliferative phenotype (*Culture, grey bars*). Expression levels were normalized to the housekeeping gene RPL18 and expressed as $2^{-\Delta Ct}$, where $\Delta Ct = Ct_{channel} - Ct_{RPL18}$. (see online methods). Each data is the mean ± SEM of 5-9 different preparations with triplicate determinations. * $p<0.05$; ** $p<0.01$; *** $p<0.001$ (All through the text). **b.** Bars plot shows the Kv1.3:Kv1.5 ratio in four human vascular beds both in contractile (white bars) and proliferative (grey bars) phenotype. The ratio was expressed as $\log 2^{-(\Delta CtKv1.3 - \Delta CtKv1.5)}$. In this scale, a value of 0 indicates equal expression (i.e., a Kv1.3:Kv1.5 ratio of 1), -2 denotes 100 times higher Kv1.5 expression than Kv1.3, and +2 Kv1.3 expression levels 100 times higher than Kv1.5. Each data point was obtained from at least 6 different vessels/cultures. **c.** The relative abundance of Kv1.3 (white) and Kv1.5 (grey) mRNA in the four preparations in both tissue and cultured VSMCs is illustrated by the pie charts.

Figure 2. Changes in the functional expression of Kv1.3 and Kv1.5 proteins during PM. a. Representative immunoblots of VSMCs lysates obtained from hRA homogenates (Tissue, T) or hRA primary cultures (C) with anti-Kv1.3 (left) or anti-Kv1.5 antibodies (right). Positive controls were brain (Br) and heart (H) lysates (Kv1.3 and Kv1.5 respectively), and β-actin was used as loading control. Bars plots show averaged data from 3-5 inmunoblots. Kv1.3 or Kv1.5 protein expression was corrected for β–actin and normalized to the amount expressed in tissue. Note the logarithmic scale. **b.** Time course of the peak current amplitude elicited by 200ms pulses to +40mV applied every 10 s in freshly dissociated (upper graph) or cultured (lower graph)hRA VSMCs. PAP-1 (100nM) or DPO (100nM) were applied to the bath solution as indicated. Representative traces at the time points labeled 1,2, and 3 are depicted in the insets. **c.** The effects of the blockers were expressed as percentage of inhibition of the current amplitude. Mean ± SEM values, n= 8-12 cells in each group. **d.** Absolute values of the Kv1.3 current density (pA/pF) obtained from contractile (n=9) and proliferative (n=12) VSMCs from renal arteries. Kv1.3 current density was defined as the 100nM PAP-1 sensitive current. **e.** Representative recording of membrane potential from a cultured renal VSMC obtained in current clamp with perforated-patch. The indicated drugs/solutions were present in the bath solution as marked with the lines.

Figure 3. a. The Kv1.3:Kv1.5 ratio (as in Figure 1), was obtained from renal explants incubated during 3 or 7 days in serum-free media or with 20% FBS, PDGF (20 ng/ml) or TGF-β (2 ng/ml). Mean±SEM, from 3 different vessels in triplicate determinations. **b, c.** Changes in the expression of Kv1.3 and KCa3.1 mRNA in cultured hRA and hSV VSMCs after 24h incubation with 20% FBS (**b**) or 100 ng/ml PDGF (**c**). The relative amount of mRNA ($2^{-\Delta\Delta Ct}$) was calculated using RPL18 mRNA as the housekeeping gene and the mRNA expression in serum-free VSMCs as the calibrator. In c, changes in the expression of cyclin A2 and calponin mRNA upon PDGF treatment were explored as internal controls for proliferation and differentiation respectively. Mean±SEM, n=4-6 experiments with triplicate determinations.

Figure 4. a. Proliferation rate in the four vascular beds studied was calculated as the percentage of cells incorporating EdU. After 48h incubation in serum-free media cells were kept during 30h in serum-free or in the presence of 5% FBS alone or in combination with 10 nM MgTx (MgTx) or 100nM PAP-1 (PAP-1). EdU reagent was added to the media during the last 6 hours of incubation. Each bar is mean±SEM of at least 6 independent experiments from at least 4 different cultures. **b.** Proliferation rate was also explored upon 30 h treatment with two different mitogens, PDGF (100 ng/ml)

and angiotensin II (AT-II, 1µM). In both cases cells were incubated with the mitogens alone or in the presence of 100 nM PAP-1. Mean±SEM, n=3. **c.** The effect of PAP-1 (100 nM) on 5% FBS or 100ng/ml PDGFinduced proliferation is represented as the percent inhibition of EdU incorporation rate in three different vascular beds. Mean±SEM, n=3-6. **d.** Effects of the selective Kv1.3 blockers PAP-1 (100 nM) and MgTx (10 nM), and the selective BK_{Ca} blockers Paxilline (500nM) or Iberiotoxin (IbTx, 100nM) and the selective KCa3.1 blocker TRAM-34 (100 nM) on PDGF-induced proliferation of hRA VSMCs. Cells were incubated during 30 h in the presence of 20 ng/ml of PDGF alone (black bars) or in the presence of the different blockers. Mean±SEM, n= 5-8 data from at least 3 different experiments.

Figure 5. a. Effects of different treatments on the PDGF-induced proliferation of hCA VSMCs. VSMCs were serum starved for 48h and then incubated 30h with 100ng/ml PDGF (control) alone or with blockers of several PDGF-activated signaling cascades at the indicated concentrations. The combined effect of these blockers with 10 nM MgTx (dark gray) or 100nM PAP-1 (light gray) was also explored. Data were normalized to EdU incorporation in control conditions. Mean±SEM of 5-20 determinations from at least three different cultures. Proliferation induced by PDGF-treatment alone and in combination with PAP-1 were internal controls for each experiment. **b.** Diagram showing the pathways explored and the targets of the blockers used. The putative location of Kv1.3 in the proliferative response is also indicated. **c.** Dose-response curves for the effect of everolimus alone (●) or in the presence of 100nM PAP-1(■) on PDGF-induced proliferation of hCA VSMCs. Data are normalized to the proliferation rate in 100 ng/ml PDGF, and the solid lines indicated the Boltzmann fit of the data. The effect of 100nM PAP-1 at each everolimus concentration (grey triangles) was estimated by subtracting both curves. Each point is mean ± SEM of 3-6 determinations.

Figure 6. Effects of TRAM-34 on hCA VSMC proliferation. VSMCs were serum starved for 48h and then incubated 30h with 100ng/ml PDGF (control). The different blockers used were also present during 30 h. The effect of TRAM-34 (100nM) was tested alone or in combination with 100nM PAP-1, 20 µM PD98059 or 1 nM everolimus as indicated. Mean ± SEM of 4-7 determinations.

Figure 7. a.**Time course of ERK1/2 activation.** hCA VSMCs in culture were serum starved for 48h and stimulated with PDGF (100 ng/ml) alone or with PAP-1(100 nM). ERK1/2 phosphorylation was assayed by immunoblotting with pERK antibody, with tubulin as loading control. The graph shows normalized data obtained from n=4 experiments. **b. Time course of the changes in $[Ca^{2+}]_i$ in response to acute application of PDGF.** hCA VSMCs were serum starved for 24h before loading with fluo-4. Traces show changes in $[Ca^{2+}]_i$ in response to a short (5 min) application of 50 ng/ml PDGF alone or in the presence of 10 nM MgTx, 100 nM PAP-1 or 1 µM U73122 during 15 min as indicated by the horizontal bar. Each trace is mean±SEM of 12-15 cells in the same plate. Data are representative of 4 similar experiments from different cultures. **c. Cyclin D1 expression in proliferating VSMCs.** Representative immunoblots from hCA VSMC lysates obtained with anti-cyclin D1, using β-actin as the loading control. VSMC cultures were serum starved for 48h before incubation for 24h with PDGF alone or together with PAP-1 (100 nM) or everolimus (0.1 nM). The bars plot shows average data from 3 similar experiments. * compared to serum-free (0%); $ $p<0.05$ compared to PDGF.

Figure 8. a. Time course of PDGF-induced proliferation of hCA VSMCs. Cells were serum starved for 48 h and then PDGF was added for 24h or added for 30 min and then cells were maintained in serum-free media up to 24 h. In both cases, the effect of the simultaneous application of 100nM PAP-1 was also explored. N=4. **b. Time-course of the inhibitory effects of PAP-1 on VSMC proliferation**. Inhibition of

VSMC proliferation induced by 100 nM PAP-1 was plotted as a function of PAP-1 incubation time. hCA VSMCs were serum starved during 48h and then incubated for 24h with PDGF (100ng/ml). PAP-1 was added at the same time than PDGF (24h incubation time) or at the indicated intervals after PDGF application (0.5, 1 6 and 12 h). The % inhibition was calculated as $(P_{PAP}*100)/P_C$ were P_{PAP} and P_C are the EdU incorporation rates in presence and absence of PAP-1 respectively. Mean ± SEM, n= 8-11 determinations from 5 independent experiments.

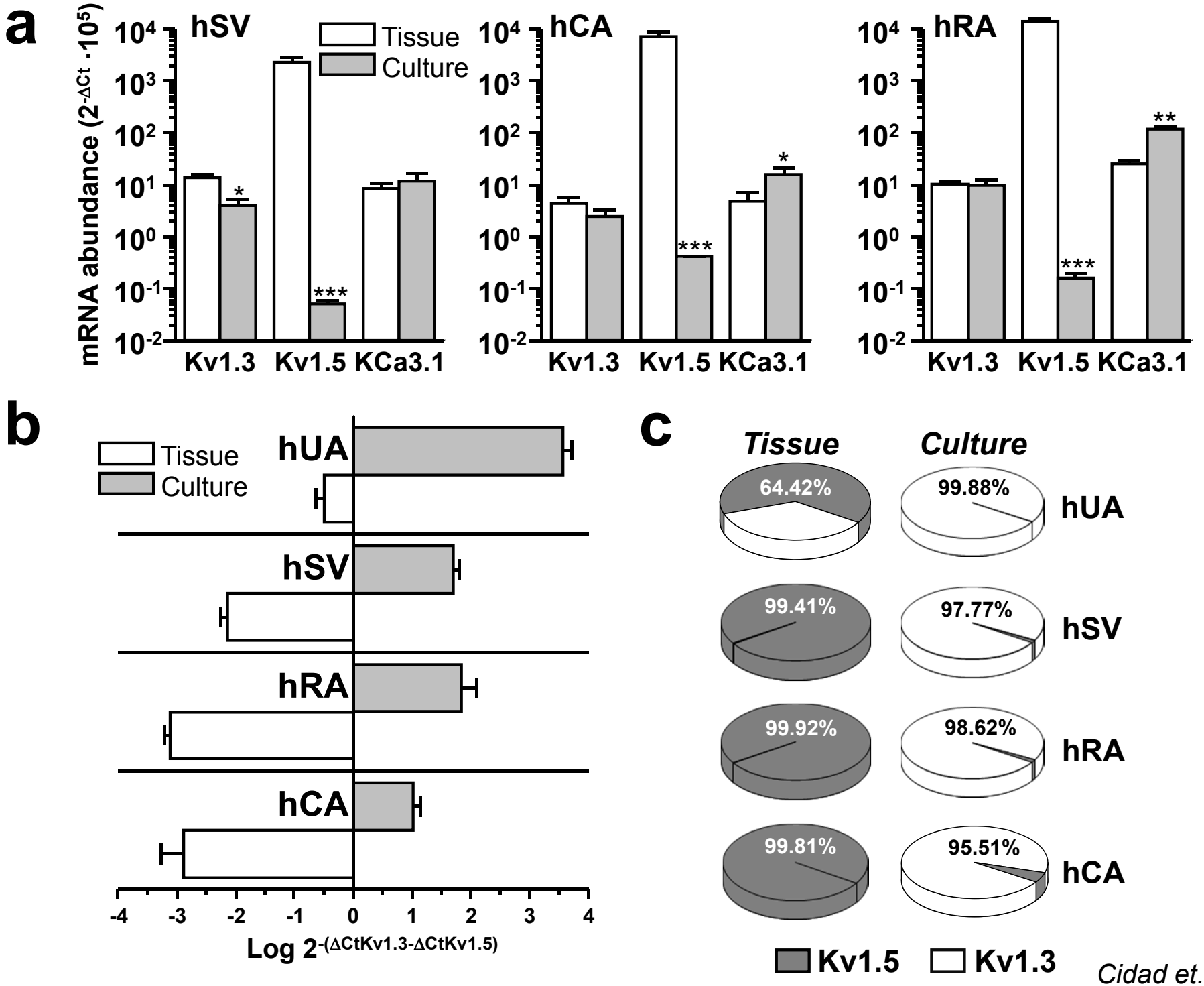

Cidad et.al. Figure 1

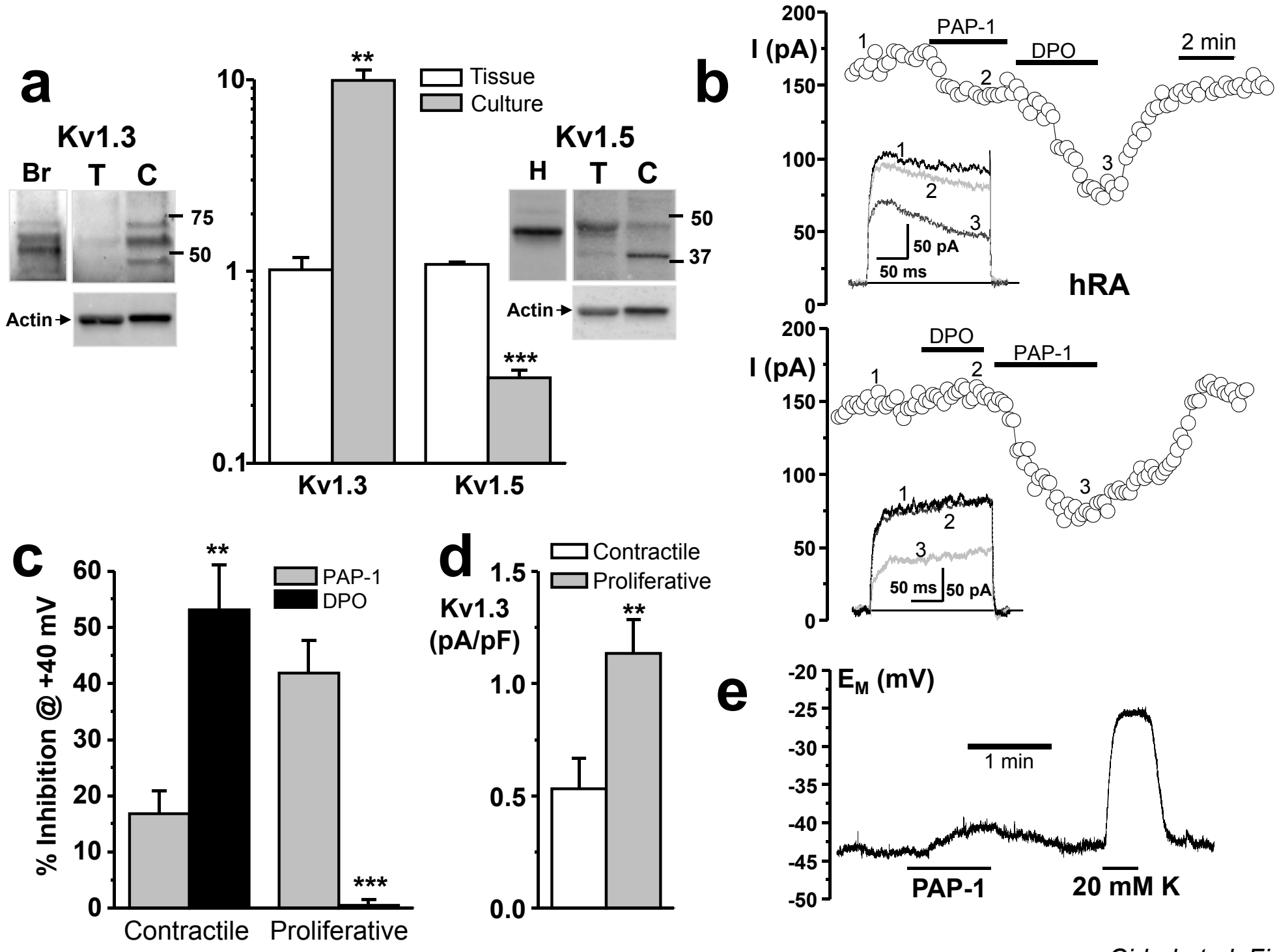

Cidad et.al. Figure 2

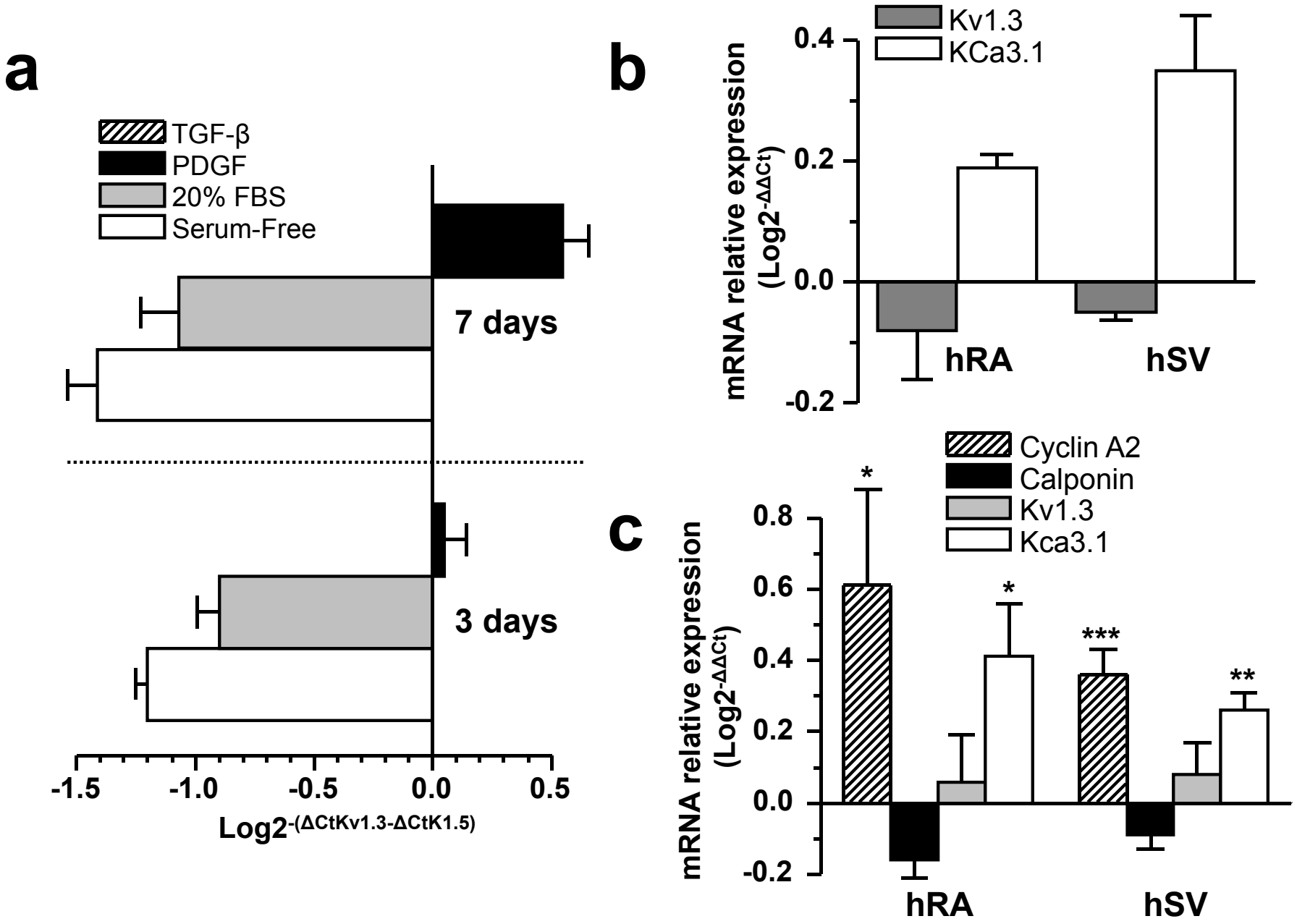

Cidad et.al. Figure 3

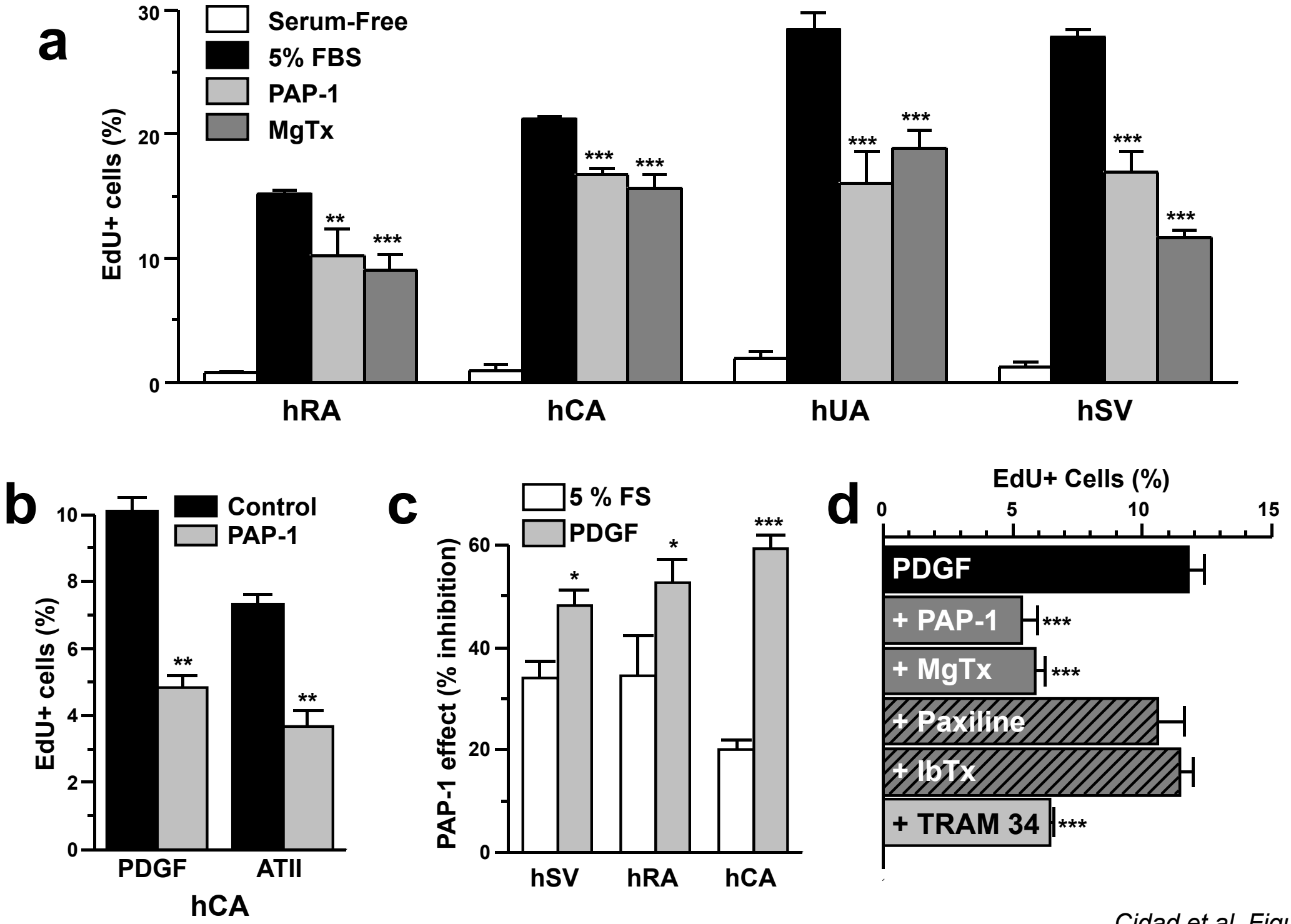

Cidad et.al. Figure 4

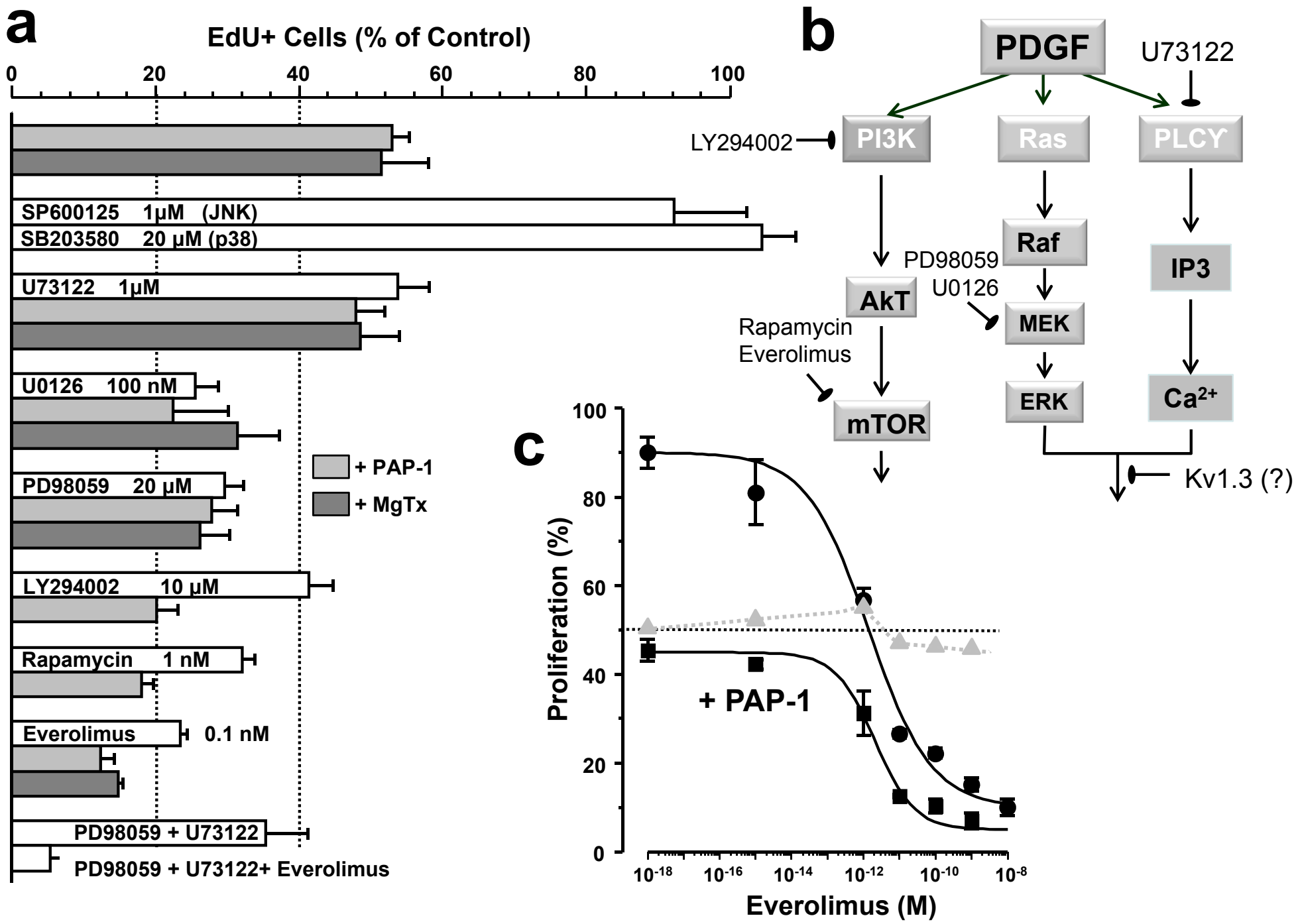

Cidad et.al. Figure 5

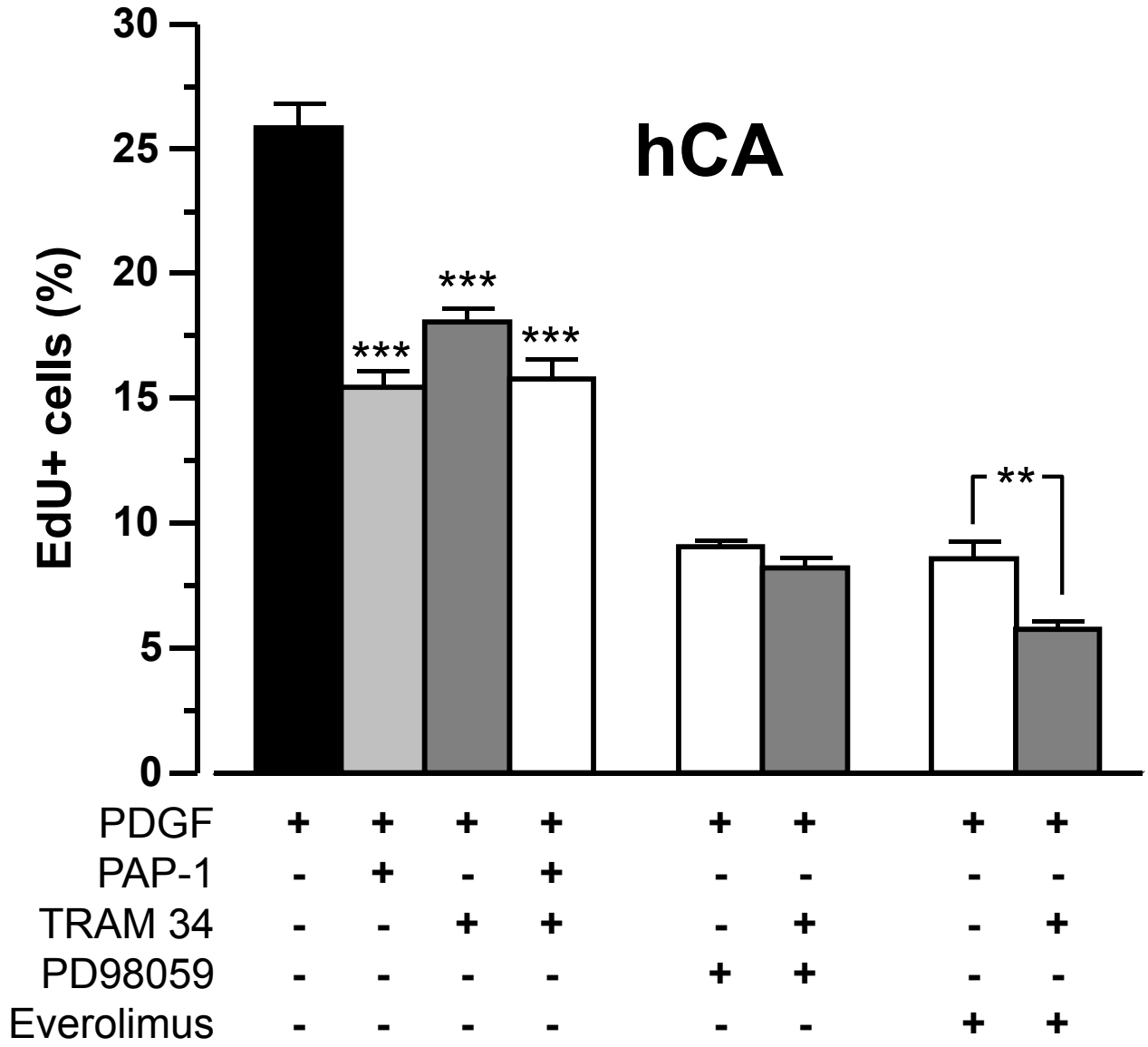

Cidad et.al. Figure 6

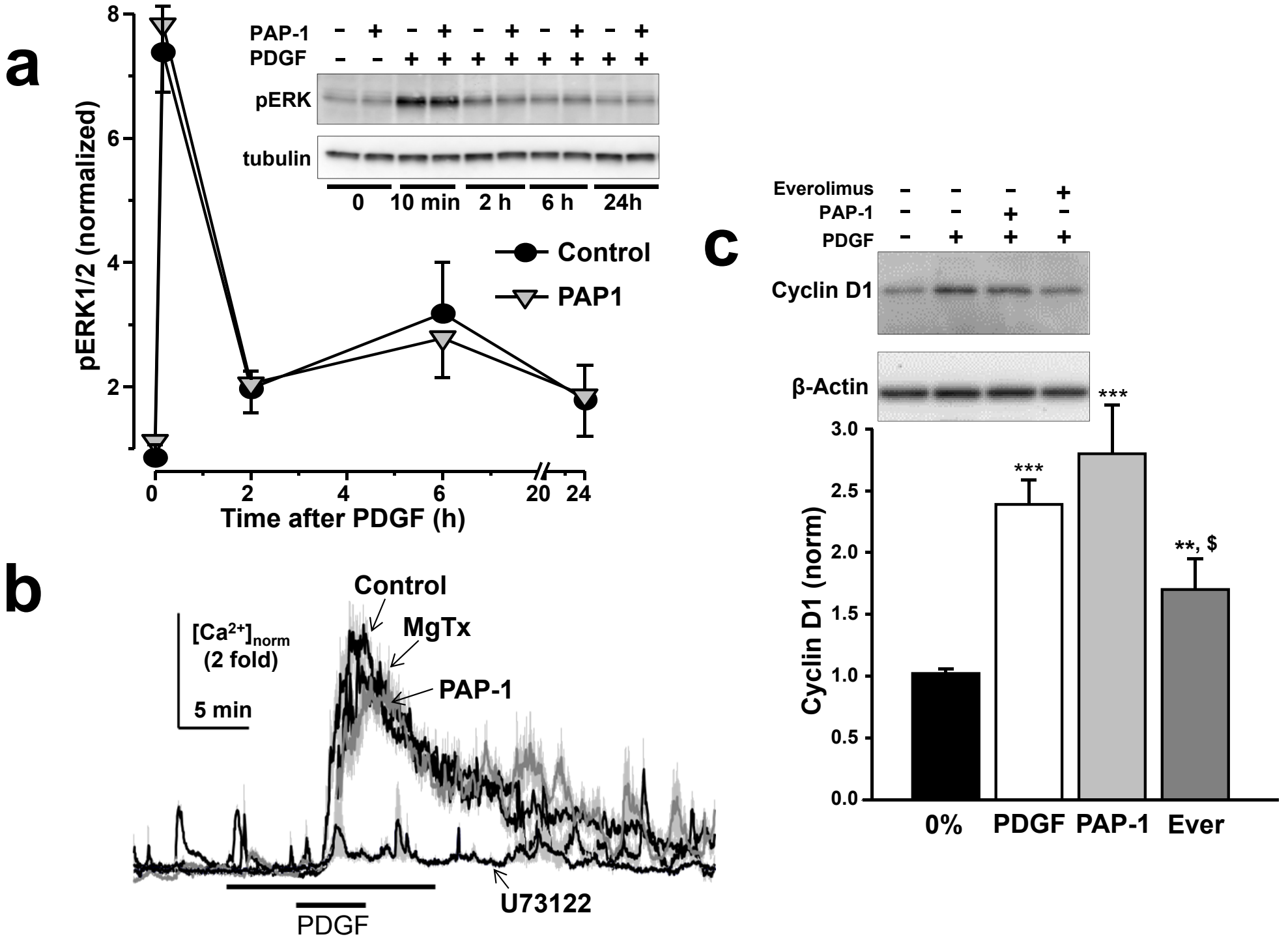

Cidad et.al. Figure 7

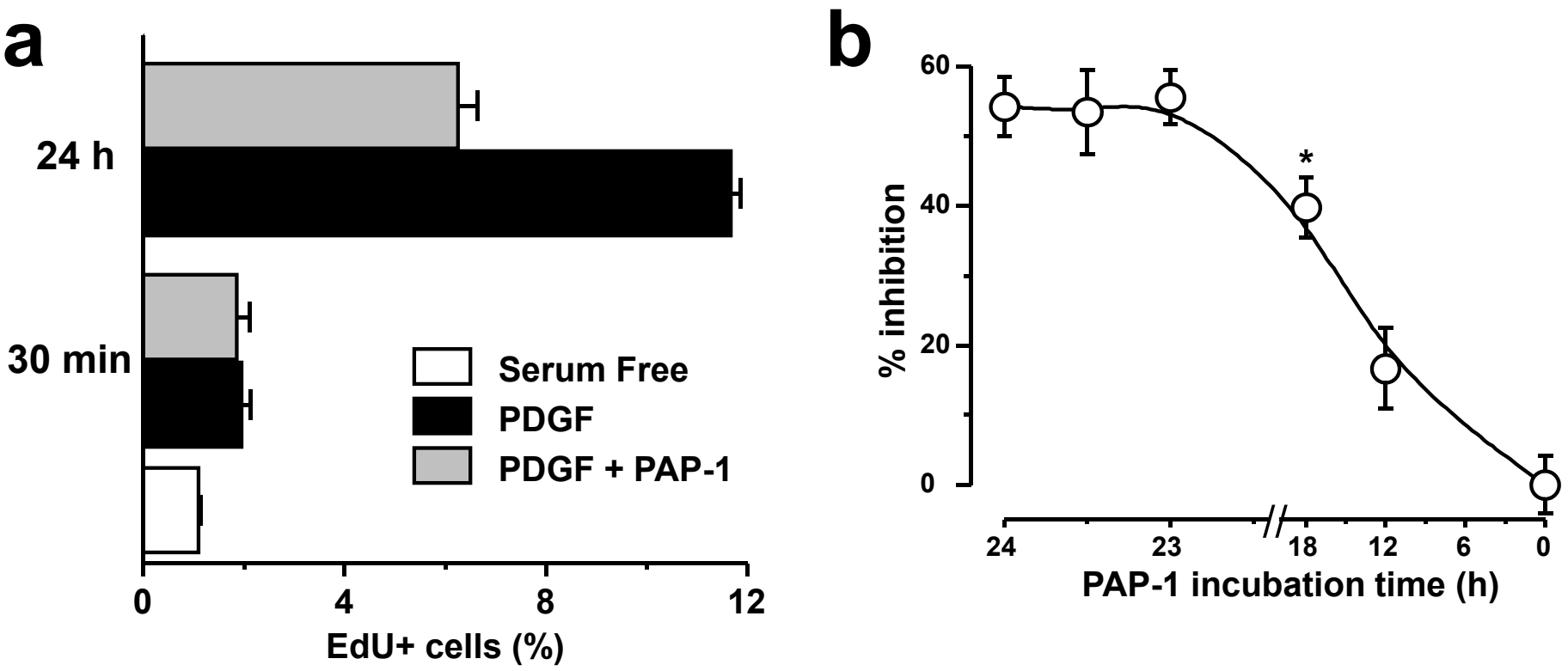

Cidad et.al. Figure 8

ONLINE SUPPLEMENTAL MATERIAL

EXPANDED MATERIALS AND METHODS

Cell culture

VSMCs were isolated from the medial layer of the vessel kept in DMEM after manual removal of both adventitia and endothelial layers under a dissection microscope. Once isolated, the muscle layer was cut in 1 mm^2 pieces that were seeded in 35 mm Petri dishes treated with 2 % gelatin (Type B from bovine skin, Sigma) or collagen (6 well multidish collagen, Thermo Scientific), in DMEM supplemented with 20 % SFB, penicillin-streptomycin (100 U/ml each), 5 µg/ml fungizone, and 2 mM L-glutamine (Lonza) at 37 ºC in a 5% CO_2 humidified atmosphere. Migration and proliferation of VSMCs from the explants was evident within 10-15 days. Confluent cells were trypsinized and seeded at 1/3 density and VSMCs were subjected to several (up to 8) passages in control medium. The composition of this media was DMEM with 5% FBS, penicillin-streptomycin, fungizone and L-glutamine as above, and supplemented with 5 µg/ml Insulin, 2 ng/ml bFGF and 5 ng/ml EGF.

Real time PCR

The samples stored in RNAlater™ were homogenized with a handheld homogenizer (Omni International Inc.). RNA from the tissue homogenates and from cultured VSMCs was isolated with TRIzol Reagent and reverse transcribed as previously described [1]. The mRNA levels of Kv1.3 (KCNA3), Kv1.5 (KCNA5), $K_{Ca}3.1$ (KCNN4) Calponin (CNN1) and A2 cyclin (CCNA2) were determined by real-time qPCR with TaqMan® Gene Expression Assays (Applied Biosystems) or with SYBR Green (see below), on a Rotor-Gene 3000 instrument (Corbett Research) using the $2^{-\Delta\Delta Ct}$ relative quantification method [2]. mRNA expression levels were normalized to an internal control, ribosomal protein L18 (RPL18) mRNA. The relative abundance of the genes was calculated from $2^{(-\Delta Ct)}$, where $\Delta Ct=Ct_{genel}-Ct_{L18}$ and the changes in expression between control VSMCs and the different experimental conditions were calculated from $2^{(-\Delta\Delta Ct)}$, where $\Delta\Delta Ct = \Delta Ct_{(experimental)}-\Delta Ct_{(control)}$, the calibrator sample is indicated in each case. In this way, data in the different experimental conditions are presented as the fold change in gene expression. For the representation of these data, the logarithm of $2^{-\Delta\Delta Ct}$ was used, so that a value of 0 means no change, positive values represent increased expression and negative values decreased expression. Total RNA from human brain (BD Biosciences) was used as positive control.

Primers sets, TaqMan probes and TaqMan® Gene Expression Assays (Applied Biosystems) employed are listed below:

KCNA3-Hs00704943_s1

KCNA5-Hs00266898_s1

KCNN4-Hs00158470_m1

CNN1-Hs00154543_m1

CCNA2: F-5'-tgatagatgctgacccatacc-3' and R-5'-atgctgtggtgctttgagg-3'

RPL18: F-5'-aactgatgatgtgcgggttc-3', R-5'-cagctggtcgaaagtgagg-3' and 5'-FAM-ctgaaggtatgtgcactgcgcgtga-BHQ1-3'

Western-blot

For Kv channel expression, vascular tissues (contractile VSMCs) or cultured VSMCs (proliferative) were harvested in RNAlater™ and homogenized proteins were recovered from organic phase created by addition of chloroform to TRIzol Reagent (Invitrogen, see manufacturer's protocol). Protein content was determined by using the Pierce™ BCA Protein assay kit (Pierce or Thermo Scientific). Samples containing 25 μg of protein, with XT Reducing Agent and XT Sample Buffer (Bio-Rad) were heated for 5 min. at 95 ºC, separated by SDS-PAGE in 10 % Bis-Tris precast gels (Criterion™ XT precast gel, BioRad) and transferred to a PVDF membrane. After blockade of the membrane with 5 % non-fat dry milk in 1 X PBST (PBS with 0.1 % Tween-20), primary antibodies were diluted in blocking solution at the final concentrations of 1:1000 and incubated for 1 h at room temperature. Then the membranes were washed with 1 X PBST and incubated with horseradish peroxidase conjugated secondary antibodies (donkey anti-mouse sc-2314 and goat anti-rabbit sc-2301, Santa Cruz Biotechnology) at final concentration 1:10000 for 1 h at room temperature. The protein signals were detected with the VersaDoc™ 4000 Image System (BioRad) with chemiluminescence reagents (SuperSignal® West Femto Chemiluminescent Substrate, Pierce Biotechnology). Protein lysates from mouse brain or heart were used as positive controls for Kv1.3 and Kv1.5 respectively, and β-actin as loading control. The relative amount of protein was calculated by densitometric analysis of the bands and normalized to their corresponding β-actin signals using Fiji (Image J) software. Primary antibodies used were mouse monoclonal anti-Kv1.3 (clone23/27, Antibody INc., USA), rabbit anti-Kv1.5 (Sigma) or mouse monoclonal anti-β-actin (ab8226, Abcam, Cambridge, UK)

For the study of ERK1/2 phosphorylation, 25,000 coronary VSMCs were seeded on 12 mm diameter plates in control medium. After 24h, cells were made quiescent with serum-free medium 48h, followed by a preincubation in the absence or presence of 100 nM PAP-1 for 1h and then stimulated with 100 ng/ml of PDGF-BB (without or with PAP-1) for 0, 10 min, 2, 6, and 24 hours. Cells were then harvested in RIPA buffer (150 mM NaCl, 1% NP-40, 0.5% sodium deoxycholate, 0.1% SDS, 50 mM Tris pH 8 and 1x protease inhibitor cocktail; Roche) to obtain protein lysates. Western-blot analysis was performed as described above, but 2,5% BSA in 1x PBST was used to block nitrocelullose membranes for p-ERK labeling. The primary antibodies used were rabbit anti p-ERK1/2 1:1000 in BSA blocking solution (Cell Signaling 9101) and monoclonal mouse anti-β-Tubulin, 1:50000 (Sigma), as loading control. For the study of cyclin D1 expression, cells were plated and incubated as above, but lysis buffer (125 mM Tris pH6.8, 2% SDS, 1 mM DTT and 1x protease inhibitor cocktail; Roche) was used to obtain cell lysates. Western-blot analysis was performed using 13% acrylamide gels and PVDF membranes. The primary antibodies used were mouse monoclonal anti CyclinD1, 1:1000 overnight at 4ºC (Clone DCS-6, NeoMarkers, Thermo Scientific) and monoclonal anti –β-Actin-peroxidase, 1:100000 (clone AC-15 Sigma) as loading control.

Electrophysiological methods

Ionic currents were recorded at room temperature (20-25ºC) using the whole-cell configuration of the patch-clamp technique. Whole-cell current recordings and data acquisition from VSMC cells were made as previously described[1;3]. Briefly, the coverslips with the attached cells were placed at the bottom of a small recording chamber on the stage of an inverted microscope and perfused by gravity with an external solution of the following composition (in mM): 141 NaCl, 4.7 KCl, 1.2 $MgCl_2$, 1.8 $CaCl_2$, 10 glucose, 10 HEPES, pH 7.4 (with NaOH). Paxilline (0.5 μM), and Tetrodotoxin (0.1 μM) were included in the bath solution to block large conductance

Ca^{2+}-dependent K^+ channels and voltage-activated Na^+ channels respectively. When freshly isolated VSMCs were used, they were placed directly in the recording chamber and allowed to settle for a few minutes before starting perfusion with the external solution. Patch pipettes were made from borosilicate glass (2.0 mm O.D., WPI) and double pulled (Narishige PP-83) to resistances ranging from 4 to 8 MΩ when filled with the internal solution, containing (in mM): 125 KCl, 4 $MgCl_2$, 10 HEPES, 10 EGTA, 5 MgATP; pH 7.2 with KOH.

Membrane potential (V_M) measurements were obtained at RT using the perforated-patch technique as previously described (Tajada et al 2012). Pipette tips were briefly dipped into a solution containing (in mM): 40 KCl, 95 KGlutamate, 8 $CaCl_2$, 10 HEPES, pH 7.2, and backfilled with the same solution containing amphotericin B (300 µg/ml). The composition of the bath solution was the same as indicated above. Electrical access to cell cytoplasm was assessed by monitoring the increase in cell capacitance. When a stable value was reached, the amplifier was switched to current-clamp mode and membrane potential was continuously recorded.

The currents were recorded using a Multiclamp 700A current and voltage clamp amplifier, filtered at 2 kHz (-3dB, 4-pole Bessel filter), and sampled at 10kHz. When leak-subtraction was performed, an online P/4 protocol was used. Series resistance was routinely compensated. Recordings were digitized with a Digidata 1200 A/D interface, driven by CLAMPEX 8 software (Axon Instruments) in a Pentium clone computer. Electrophysiological data analyses were performed with the CLAMPFIT subroutine of the PCLAMP software (Axon) and with ORIGIN 7.5 software

Intracellular calcium measurements:

For intracellular calcium measurements, coronary VSMCs were seeded on square cover slips with fibronectin and after 24 h cells were loaded with 2 µM of the fluorescent Ca^{2+} indicator Fluo-4-AM (Molecular Probes, Invitrogen, Oregon, USA) for 1 h at room temperature in the perfusion chamber. Then VSMCs were washed, the perfusion/recording chamber was placed on the stage of an inverted microscope and perfused by means of a peristaltic pump with the control solution, Tyrode solution, of the following composition (in mM): 140 ClNa, 5 ClK, 2 Cl_2Ca, 1.1 Cl_2Mg, 5 Glucose, 10 Hepes, (pH 7.4). Cells were perfused 20-30 min at a constant flow of 1 ml/min with Tyrode solution before stimulation with 50 ng/ml PDGF for 5 min. Blockers (100 nM PAP-1, 10 nM Mgtx or 1µM U73122) were present from 5 min before to 5 min after PDGF stimulation. For the study of the effects of PAP-1 on Ca^{2+} mobilization from intracellular stores, cells were treated with 10 µM ciclopiazonic acid (CPA) and bathed in a 0 mM Cl_2Ca, tyrode solution to deplete intracellular Ca^{2+}. After that, in the continuous presence of CPA, intracellular Ca^{2+} changes in response to short applications of 2 mM Cl_2Ca tyrode solutions were explored, and the effect of Kv1.3 blockers on these changes was also investigated. At the end of the experiment cells were exposed to 2 mM of the protonophore FCCP followed by 20 µM of Ca^{2+} ionophore ionomycin to determine Fmax.

Intracellular calcium images were acquired using an inverted microscope, Eclipse TE (Nikon, Tokyo, Japan), equipped with a Nikon CFI S Fluor (40X, NA=1.30) oil immersion objective and a Sensi Cam (PCO AG, Germany) camera. Images were acquired using Imaging Workbench 4.0 image software. Background-subtracted fluorescence signals were converted to concentration units using the “Fmax” equation [4].

Proliferation assays

VSMCs at passages 3-8 were seeded onto round poly-l-lysine coated coverslips placed in 12 mm wells at a density of 25,000 cells/well. Cells were maintained in control

medium for 24 h and synchronized in serum free (SF) medium during 48 h. Then, a proliferative stimulus (PDGF or FBS) was added alone or in combination with the drugs tested (ion channel blockers or specific inhibitors of the signaling pathways studied). 24 h post treatment, the percentage of cells at the S phase was quantified using EdU (5-ethynyl-2´-deoxyuridine) incorporation for an additional period of 6h with a commercial kit (Click-iT® EdU Imaging Cell Proliferation Assay, Invitrogen). Finally, cells were incubated with Hoechst before mounting with Vectashield (Vector Laboratories Inc., Burlingame, CA). EdU incorporation was visualized with an immunofluorescence microscopy (Nikon) at the corresponding wavelength depending on the Alexa Fluor® used and expressed as the percentage of the total cell number stained with Hoechst. In each experiment, this percentage was obtained from the average of 10 to 20 different fields per coverslip, selected in a blind manner, and triplicates were made for each condition.

Data analysis

Pooled data are expressed as mean ± standard error of the mean (SEM). Statistical comparisons between groups of data were carried out with the two-tailed Student t test for paired or unpaired data, as appropriate, and values of $p<0.05$ were considered statistically different.

References

1. Miguel-Velado E, Moreno-Dominguez A, Colinas O, Cidad P, Heras M, Perez-Garcia MT, López-López JR. Contribution of Kv Channels to Phenotypic Remodeling of Human Uterine Artery Smooth Muscle Cells. *Circ Res*. 2005;97:1280-1287.

2. Livak KJ, Schmittgen TD. Analysis of relative gene expression data using real-time quantitative PCR and the 2(-Delta Delta C(T)) Method. *Methods*. 2001;25:402-408.

3. Moreno-Dominguez A, Cidad P, Miguel-Velado E, Lopez-Lopez JR, Perez-Garcia MT. De novo expression of Kv6.3 contributes to changes in vascular smooth muscle cell excitability in a hypertensive mice strain. *J Physiol*. 2009;587:625-640.

4. Maravall M, Mainen ZF, Sabatini BL, Svoboda K. Estimating intracellular calcium concentrations and buffering without wavelength ratioing. *Biophys J*. 2000;78:2655-2667.

ONLINE SUPPLEMENTAL FIGURES

Online supplemental figure I. **A.** Representative immunoblots of VSMCs lysates obtained from hSV homogenates (Tissue, T) or hSV primary cultures (C) with anti-Kv1.3 (left) or anti-Kv1.5 antibodies (right). Positive controls were brain and heart lysates (Kv1.3 and Kv1.5 respectively) and β-actin was the loading control. Bars plots

show averaged data from 3-5 inmunoblots. Kv1.3 or Kv1.5 protein expression was corrected for β–actin and normalized to the amount expressed in tissue. B. The functional expression of Kv1.3 and Kv1.5 was explored in cultured VSMCs from hSV and hRA. The plot shows the percent inhibition of the peak current amplitude at +40 mV elicited in the presence of selective blockers of Kv1.3 (PAP-1 100nM and MgTx 10nM) and Kv1.5 (DPO 100nM). Each bar is mean ± SEM of 8-12 cells.

Online supplemental figure II. Dose –response curve for the effects of PDGF on the rate of VSMC proliferation. hRA VSMC were serum-starved for 48 h and then incubated for 30 h in a serum free-media (0% FBS), with the indicated concentration of PDGF, or with two different concentrations (5% and 20%) of FBS. EdU reagent was added during the last 6 h of this incubation. Each bar/data point is the mean ± SEM of 5-14 determinations obtained in 2-5 independent experiments from different cultures. The solid line represents the fit of the data to a logistic function.

Online supplemental figure III. Dose–response curve for the inhibitory effect of PAP-1 on hCA VSMC proliferation. EdU incorporation was measured after 30 h incubation in the presence of 100 ng/ml of PDGF alone or in combination with the indicated PAP-1 concentrations. During the last 6 h EdU reagent was present in the incubation media. The effect of PAP on proliferation rate was expressed as % Inhibition, and calculated as $(P_{PAP}*100)/P_C$ were P_{PAP} and P_C are the EdU incorporation rates in presence and absence of PAP-1 respectively. Each data point is the mean ± SEM of 4-6 determinations. The fit of the data to a logistic function (solid line) provided and estimated IC50 of 1,8 nM.

Online supplemental figure IV. Effect of PAP-1 on calcium transients elicited by emptying intracellular calcium stores. hCA VSMCs were superfused with a nominally calcium free media and intracellular stores were fully depleted with 10 μM ciclopiazonic acid (CPA). Calcium transients were induced by perfusing the cells with a solution containing 2 mM Ca^{2+}, before, during and after applying 100 nM PAP-1, as indicated by the horizontal bars. The magnitude of the calcium transients was integrated over time, and results obtained in several cells from different cultures are depicted as box plots as an inset. No differences between control transients and those obtained in the presence of PAP-1 were evident.

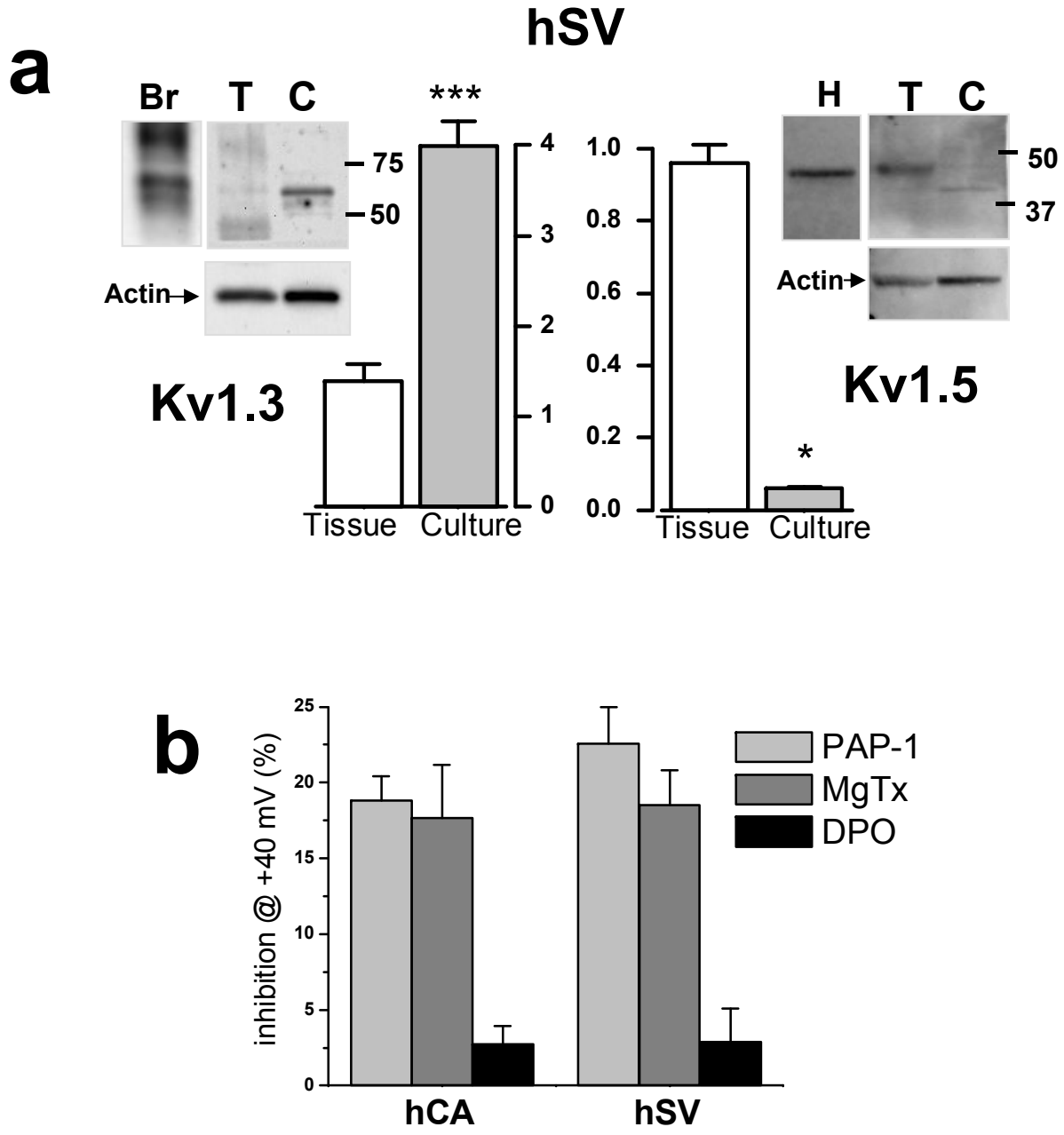

Online supplemental figure I

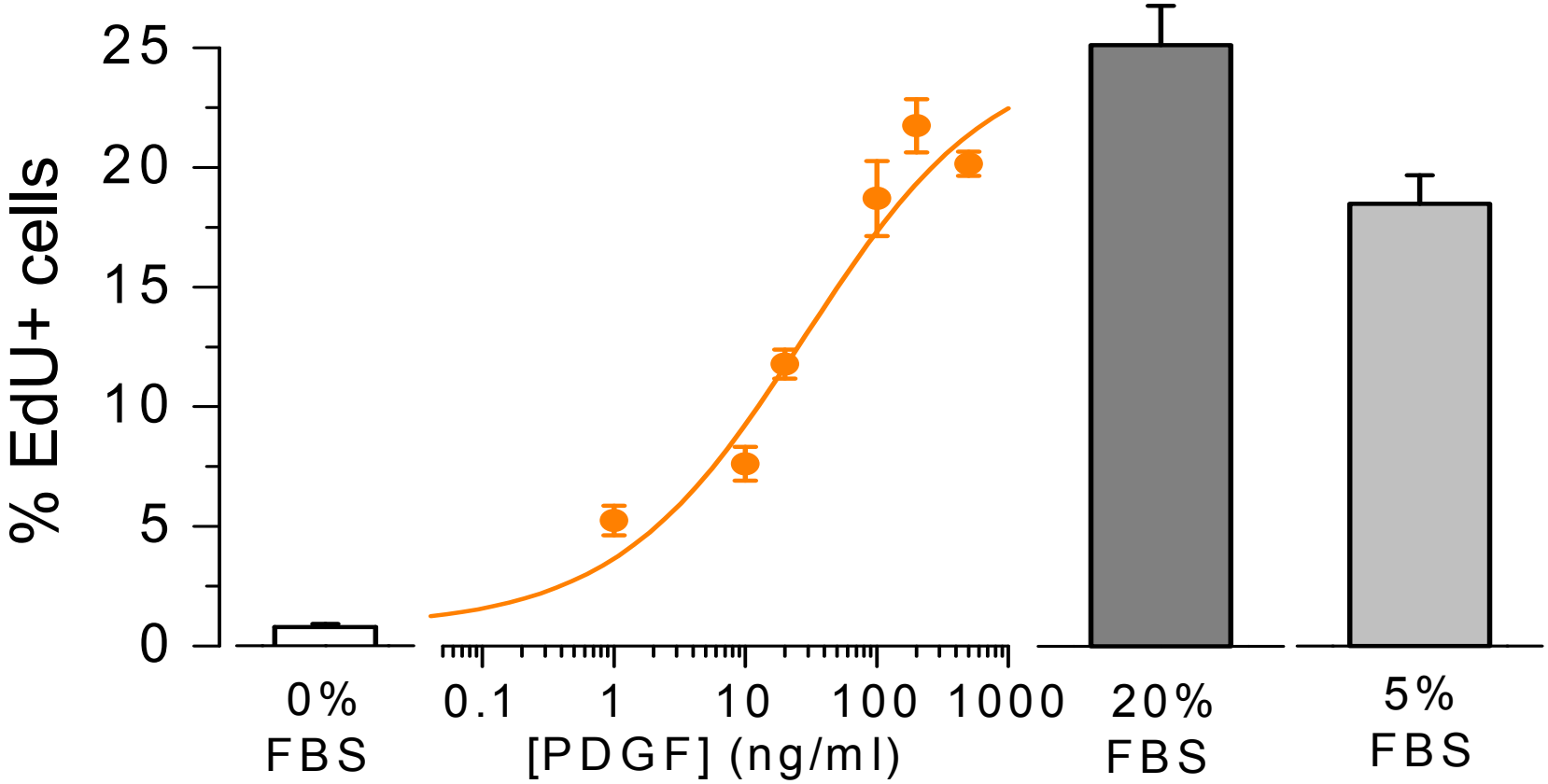

Online supplemental figure II

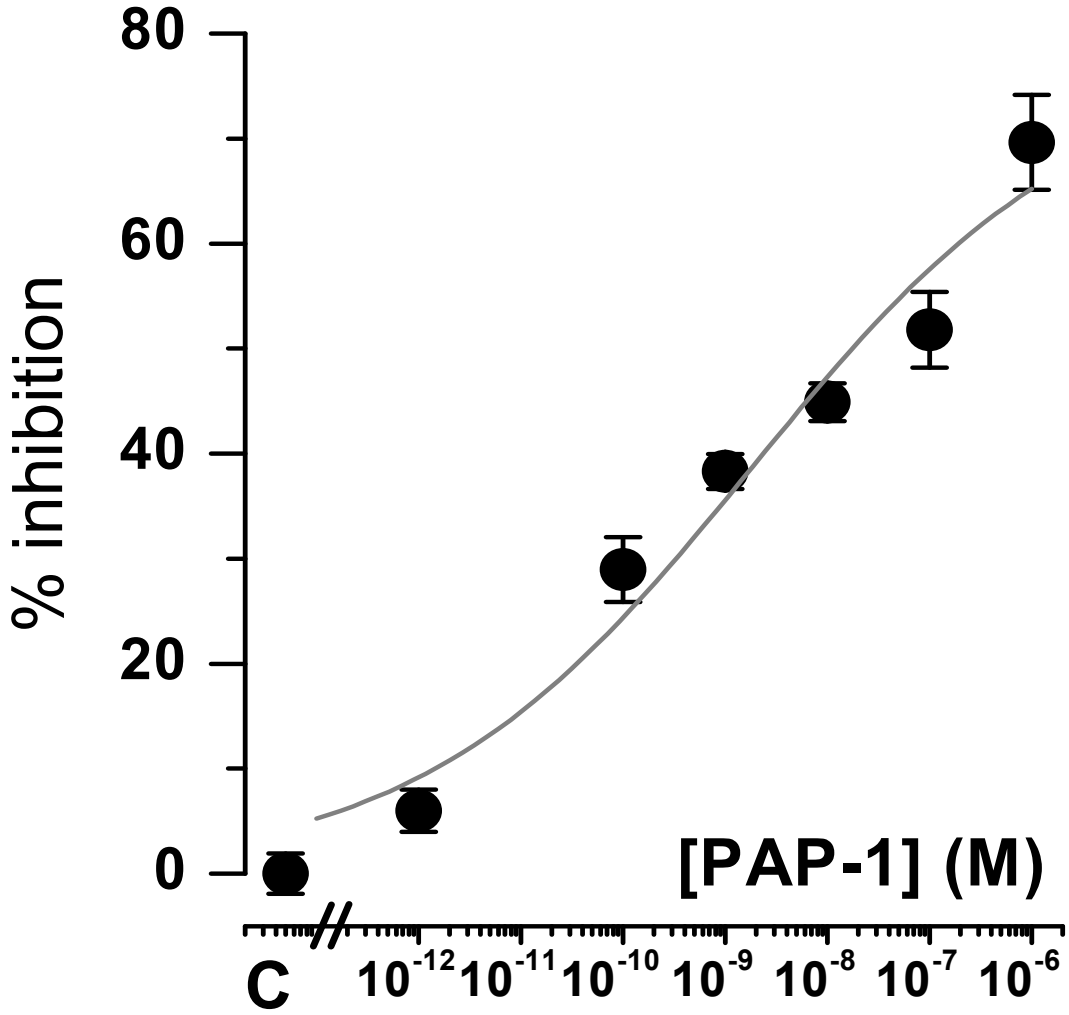

Online supplemental figure III

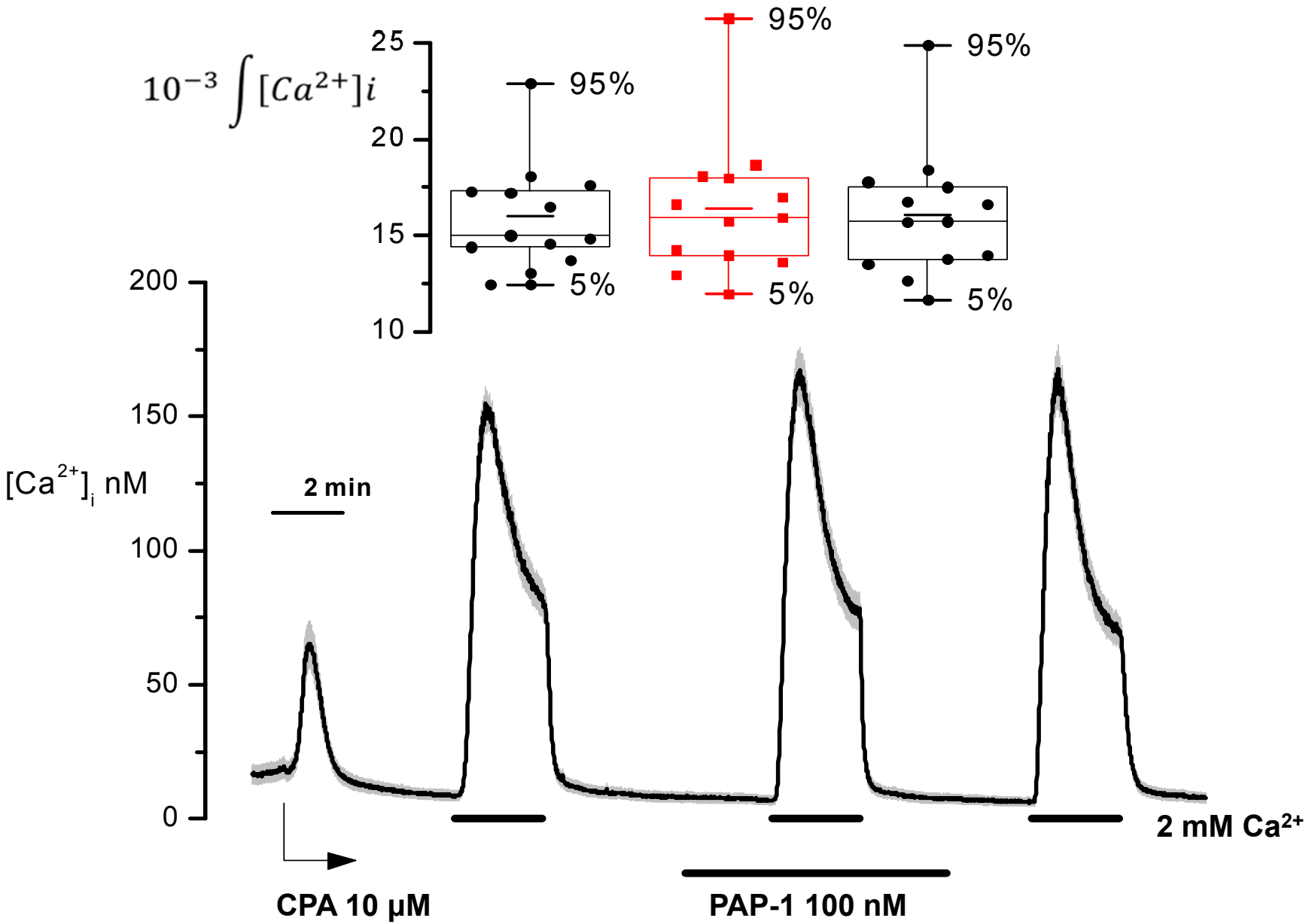

Online supplemental figure IV